

2-1-3 Survey Method

As we send an electric current into the earth, various electric chemical phenomena occur in the medium that composes the ground. IP method measures the following two phenomena.

“Over Voltage Effect”

The electric double layers occur on the surface of sulfide minerals or conductive metals due to electric current, and the charged electricity is discharged to the reverse direction when the current is cut. This phenomenon is of the combined effect of the ion conduct and electron conduct. The electron conductive minerals take place this phenomenon, and are good targets for the IP method.

“Polarization of Clay Mineral”

Common rocks are slightly polarized due to electric current, because of the membrane polarization of a small-amount of clay minerals in rock cavities. Montmorillonite shows the greatest membrane polarization, and kaolin shows low. The membrane polarization shows the greatest value when clay mineral content ratio is about 5 per cent, but decreases its value around such content.

The polarization value is much smaller compared with that of the Over Voltage Effect.

2) Measuring Method

The applied measuring method is the time-domain induced polarization method (TDIP method), and the dipole-dipole for electrode arrangement, the electrode interval 100 meters, the electrode isolation factor $n=1$ to 5, and the survey line separation 200 meters.

The intermittent direct current, on/off 2.0 sec, has been employed between the current electrodes C1 and C2, and the primary potential V_p and damping secondary potential V_s have been measured right before and after the current interruption. The apparent resistivity is measured by the primary potential during current introduction, and the chargeability is measured by the damping secondary potential.

Figure II-2-1-3 shows the concept of the operation, and Figure II-2-1-4 shows the concept of the measuring method. The sampling time is t_4 to t_{14} after current interruption, as shown in Figure II-2-1-4.

The IP effect measurement value by the time domain method is called “chargeability, and represented by V_s/V_p [mV/V]. The chargeability is the integral data of 450 to 950 [msec].

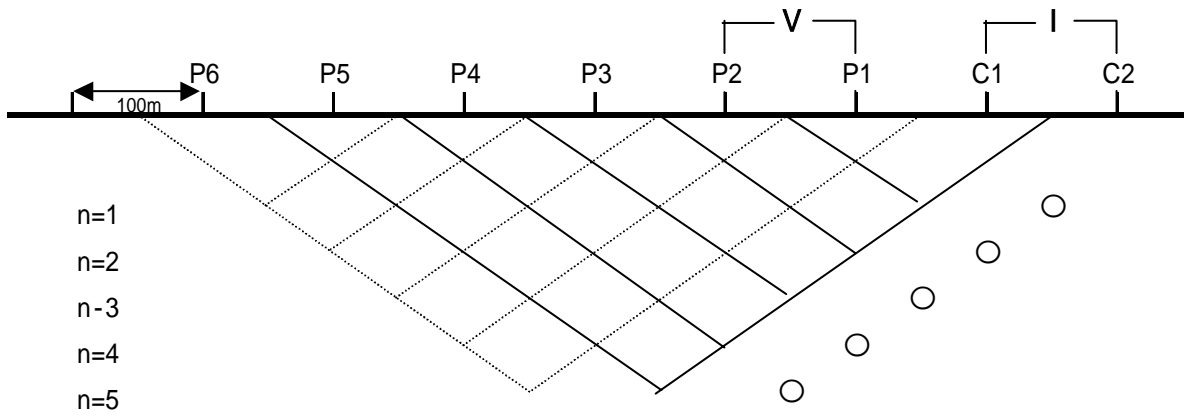


Fig. -2-1-3 Concept of operation

chargeability[mV/V]

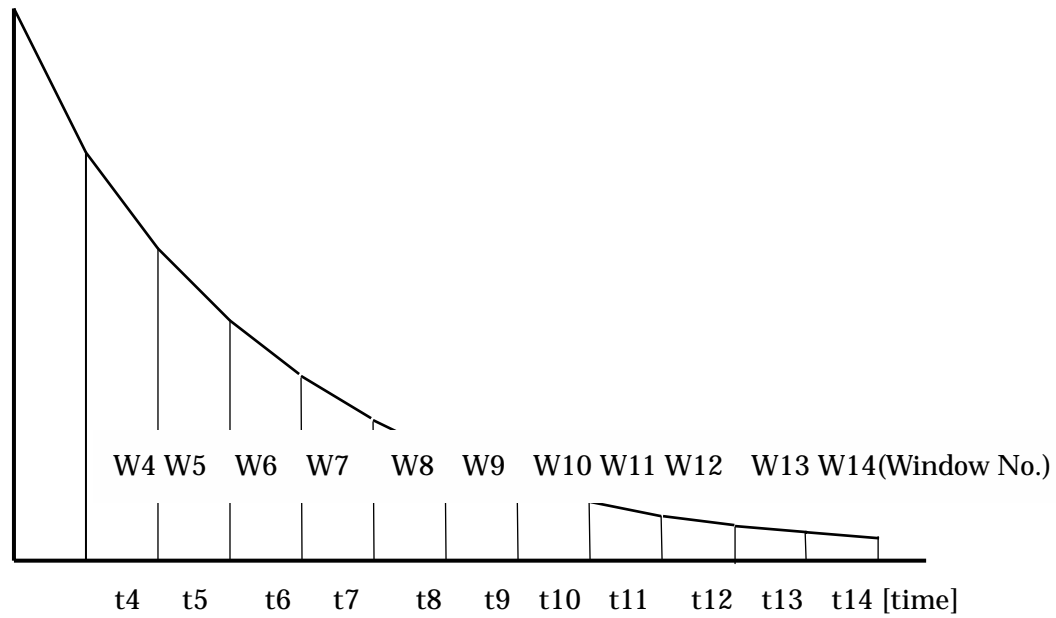


Fig. -2-1-4 Concept of the method of measurement

Table -2-1-3 List of sampling time

Window #	W4	W5	W6	W7	W8	W9	W10	W11	W12	W13	W14
Mid-point (msec)	60	90	130	190	270	380	520	705	935	1230	1590
Width (msec)	20	40	40	80	80	140	140	230	230	360	360

3) Equipment used

Table II-2-1-4 shows the specification of IP survey instrument used for the survey.

Table -2-1-4 Specification of IP survey instrument

Equipment	Type	Maker	Specication	Amount
Transmitter	CH-97T,P	CHIBA	Max.Output Current 60A	1
	CH-98T,PA	Electro Inc.	Max.Output Volt. 880V	1
Engine Generator	ET-4500	HONDA	Max.Power 4.5KW 3 220V	2
Receiver	IPR-12	SCINTREX	8ch. 14Window Input Range:50 μ Vto 14V	2
Electrode		ASK System	PbCl	12
Measuring	Pocket c ompass	USHIKATA		2
	100m Esron tape			4
	GPS	GARMIN		3
Communication Device	TH-42	KENWOOD	Max. Power:5W	12

2-1-4 Analytical Method

The two dimension inversion analysis combined the model calculated by the finite factor analysis and the auto-analysis by the nonlinear least squares method has been used for the study. In this method, the cross section showing the topography is divided into some blocks. These blocks are given their resistivity values and chargeability values, and the resistivity and chargeability structures are presented, then the model calculation by the finite factor method is performed.

Finally, the minimum resistivity structure and chargeability structure are gain by the auto-repeating analysis applied the last squares method. RES2DINV of GETOMO SOFTWARE has been used for the analysis.

2-1-5 Survey result

2-1-5-1 Mesurment Result

Figures II-2-1-7 to II-2-1-39 show the cross sections and planes of the apparent resistivity, charge rate, and metal factor.

The measurement result are principally shown in data of the short electrode spacing ($n=1, 2, 3$) due to the dipole-dipole configuration. If wide spacing is adopted, then the shallow part affection reaches to the deeper.

1) Azzouz district (Figures II-2-1-7 to II-2-1-27)

The resistivity is very variable from 8 to 1,300 ohm-m. The chargeability from 1 to 55 mV/V..

The characteristic of the apparent resistivity distribution is generally classified as follows.

1) General distribution of the young sediments

The low apparent resistivity zone, lower than 50 ohm-m, in the east to southeastern district (survey lines o, a, b, c). It tends to be low resistivity in the shallow part, but higher resistivity to the deep.

2) Nearby resumed tectonic lines

The low apparent resistivity zone, lower than 50 ohm-m, in the central north district (survey lines g, h, i, j, k). It tends to be low resistivity from the shallow to deep.

3) Other than 1) and 2)

The Paleozoic outcrop area. The shallow part is of relatively high resistivity, higher than 100 ohm-m. The deep part is of complicated distribution of low and high resistivity. The relatively deeper survey lines g(No.7,8), h(No.10,11), I(No.12,14), j(No.15,17), k(No.14,16) show a northeast to southwest trending low resistivity zone.

The chargeability anomaly generally continues to the west, centering its maximum value around the survey points g(N.7), to k(No.17). The area showing the maximum chargeability is corresponded with the ground magnetic anomaly zone.

2) Hbibbi district (Figure II-2-1-28)

The young sediments are distributed in this area. The resistivity ranges 30 to 80 ohm-m, small variation. The charge is low, ranging 3 to 15 mV/V. A weak anomaly exists around No.11, corresponding to the buried land with residual soil.

3) Harch district (Figure II-2-1-29)

The young sediments, fluvial deposit, overlies the area. The resistivity ranges 30 to 170 ohm-m, high in the shallow and low in the deep. The chargeability is low, ranging 3 to 8 mV/V.

4) Maouch district (Figure II-2-1-30)

The young sediments, fluvial deposit, overlies the area. The resistivity ranges 20 to 70 ohm-m. The chargeability is low, ranging 1 to 13 mV/V.

5) Khefawna district (Figure II-2-1-31)

The young sediment overlies in this area. The resistivity ranges 10 to 200 ohm-m, tending to higher in the deep. The chargeability is low, ranging 3 to 12 mV/V.

6) Talzelt-N district (Figure II-2-1-37 to 39)

The young sediments overlies in this area. The survey line has been set an area showing relatively low magnetic anomaly zone. The resistivity ranges 10 to 120 ohm-m, showing slightly higher in some deep parts. The charge rate is low, ranging 2 to 9 mV/V.

2-1-5-2 Analytical Result

Figures II-2-1-40 to II-2-1-77 show the cross sections and planes for the resistivity, chargeability, and metal factor from the result of the analysis.

Azzouz district (Figure II-2-1-40 to 65)

The resistivity ranges 2 to 2,600 ohm-m, and the chargeability ranges 2 to 78 mV/V. The survey district has been underlain by three zones of low resistivity structure, lower than 50 ohm-m, as follows.

- 1) The low resistivity structure continues from the surface to the depth of 100 meters of the survey lines o, a, b and d. The deeper part under 100 meter is of the high resistivity structure, higher than 200 ohm-m. It is analyzed that the high resistivity structure trends from the west side toward the east deeper part, which is correlated with the young sediments.
- 2) The low resistivity structure is distributed in the northern side of the survey lines h, i, j and k, presumably extending from the shallow to the deep part. Tectonic structure line, probably fault, is supposed the end of the survey lines No.2 and 3.
- 3) The resistivity structure is continuously recognized from the area near the survey

lines g(No.7), h(No.19), I(No.13), j(No.16), and k(No.16) in the depth of 100 meters to the deeper part. The zone is expanded northeast to southwest, further to the deeper part.

The chargeability structure is relatively low in the shallow part, 50 to 100 meters deep, presumably reflecting distribution of the young sediments.

The relatively high charge rate structure is situated around the survey lines j and k, point No.14 in the depth of about 50 meters, and the northeast to southwest trend is clear in the depth of 80 meters. It tends to show higher chargeability in the deeper part below 140 meters level. The divided charge rate structure by some complex tectonic lines is clearly seen

Metal factor

The measured chargeability for the resistivity of sulfide minerals is significantly varied due to the low resistivity change in its surrounding area. It is difficult to completely eliminate affection of resistivity due to nonlinear and complex change responding complicated geological structure. The metal factor shown here is presented as “chargeability / resistivity * 100”.

The metal factor is the highest, 1,222, in the survey line k, points No.15 and 16. The northeast to southwest extending anomaly zone is seen in the area along the survey lines g(No.7), h(No.10), I(No.13), j(No.16), and k(No.16) below the depth of 110 meters. The area is corresponded with a part of the magnetic anomaly zone.

Habibi district (Figure II-2-1-66)

The resistivity ranges 15 to 200 ohm-m, and the charge rate range 2 to 20 mV/V. Most of the resistivity except a part of near the surface is low, 20 to 30 ohm-m. It presumably reflect the thick young sediments, fluvial deposit. The weak anomaly of the charge rate is presumably corresponded with a part of buried residual soil including some waste material. No IP anomaly exists here.

Harch district (Figure II-2-1-67)

The resistivity ranges 25 to 480 ohm-m, and the chargeability ranges 2 to 11 mV/V. The high resistivity about 500 ohm-m reflects the near-surface gravel layer. The resistivity structure of 100 ohm-m exists along the point No.11 and 12. No IP anomaly exists in this area.

Maouch district (Figure II-2-1-68)

The resistivity ranges 14 to 122 ohm-m, and the charge rate ranges 1 to 14 mV/V. the resistivity structure is of lower in the deeper. The chargeability tends to slightly higher in the deeper. The young sediments presumably thick in the area. No IP anomaly exists in this area.

Khefawna district (Figures II-2-1-69 to 74)

The resistivity ranges 11 to 217 ohm-m, and the charge rate ranges 4 to 14 mV/V. The resistivity structure is of some dome-like shape, lowest in the surface and highest in the deep part of the point No.8, and tends to higher in deeper. No IP anomaly exists here.

Talzelt district (Figures II-2-1-75 to 77)

The resistivity ranges 10 to 120 ohm-m, and the charge rate ranges 2 to 9 mV/V. The resistivity structure shows tends to higher in the deep. No IP anomaly exists in this area.

Table II-2-1-4 shows the summary of the result.

Table II-2-1-4 Result of the IP survey

Azzouz Area	Characteristic of analysis result
Resistivity, chargeability:	2 to 2,600 ohm-m, 2 to 78 mV/V
Low resistivity structure:	<50 ohm-m
1)	East to southeast side survey lines o, a, b, c, d, around 100 meters from the surface. Thick young sediments in the eastern side.
2)	Extending from the shallow to deep in the north side of survey lines h, i, j, k. Complicated distribution in survey lines j, k, No.6, 7. Some tectonic structure (fault) in the end of survey line No.2, 3.
3)	Survey lines g(No.7, h(No.10), I(No.13), j(No.16), k(No.16), extends from the depth 100 meters to the deeper, elongate NE - SW.
Charge rate structure:	
Low chargeability structure	Shallow part (50 to 100m), relatively broad and low. Reflect young sediments distribution
Relatively high chargeability structure	Depth 50m, survey line j, k, No.14 Depth 80m, survey line d to r, elongate NE-SW.
High chargeability structure	Depth >140m, higher in deeper Deeper: complex divided structure
Metal factor	Depth >110m, g(No.7), h(No.10), i(No.13), j(No.16), k(No.16), elongate NE-SW IP anomaly
Hbibi Area	Characteristic of analysis result
Resistivity, chargeability:	15 to 200 ohm-m, 2 to 20 mV/V
Resistivity structure:	20 to 30 ohm-m except surface. Reflect thick young sediments (fluvial).
Chargeability structure:	No. 11; reflects residual soil (incl. waste), weak anomaly , No IP anomaly.
Harch Area	Characteristic of analysis result
Resistivity, chargeability:	25 to 480 ohm-m, 2 to 11 mV/V.
Resistivity structure:	Surface 500 ohm-m, reflect gravel layer. No.11,12 100 ohm-m in deep No IP anomaly
Maouch Area	Characteristic of analysis result
Resistivity, chargeability:	14 to 122 ohm-m, 1 to 14 mV/V.
Resistivity structure:	Lower in deeper
Chargeability:	Slightly higher in deeper, reflect thick young sediments. No IP anomaly.
Khefawna Area	Characteristic of analysis result
Resistivity, chargeability:	11 to 217 ohm-m, 4 to 14 mV/V.
Resistivity structure:	Surface low, dome-like high anomaly zone, highest at No.8. No IP anomaly.
Talzelt Area	Characteristic of analysis result
Resistivity, chargeability:	10 to 120 ohm-m, 2 to 9 mV/V.
Resistivity structure:	Slightly higher in deeper. No IP anomaly

2-1-6 Consideration

The result of the analysis in this study has revealed that some low resistivity and high chargeability IP anomaly zones in the Azzouz district (MJTK-IP04-1), however, no IP anomaly has been detected in the Hbibí district (MJTK-IP04-2), Harch district (MJTLK-IP04-3), Maouch district (MJTK-IP04-4), Khefawna district (MJTKIP04-5), and Talzelt district (MJTL-IP-06).

1) Airborne and ground magnetism

The setting of the IP survey lines has been planned based on the detail ground magnetic survey result in the Azzouz, Khefawna, and Talzelt districts previously done by BRPM. The plan for other districts has been made based on the first year's airborne magnetic survey result.

The result of the airborne and ground magnetic surveys shows relatively gentle magnetic variation for the Hbibí, Harch, Maouch, Khefawna, and Talzelt districts, but complicated variation for the Azzouz district.

Some tectonic lines has been presumed in the northern and eastern parts of the Azzouz district due to the great magnetic variation.

2) Resistivity

The resistivity of the young sediments distributed in the whole area of the survey districts is presumably lower than 50 ohm-m. The sediments generally shows a horizontal stratiform structure, based on the resistivity structure analysis, and that of the Hbibí, Harch, Maouch, Khefawna, and Talzelt districts is more than 150 meters in thickness, and That of the Azzouz district is presumably thicker in the eastern part.

Other low resistivity structures, lower than 50 ohm-m, in the Azzouz are recognized in the northern district around the survey lines (i,j,k), g(No.7), h(No.10), i(No.13), j(No.16), and k(No.16). The resistivity structure in the northern district is presumably correlated with the tectonic line, probably extending to the depth.

The low resistivity structure in the survey lines g(No.7), h(No.10), I(No.13), j(No.16), and K(no.16) is presumably of a platy shape, extending northeast to southwest and dipping almost vertically to the depth.

3) Chargeability

The charge rate measured is maximum 20 mV/V in the Hbibí, Harch, Maouch, Khefawna, and Talzelt districts, and no anomaly exists in this area. The charge rate is maximum 78 mV/V in the Azzouz district.

The relatively high chargeability structure is clearly seen around the No.14 of the survey lines j and k at the depth of 50 meters and in the survey lines d to r at the depth of 80 meters, extending northeast to southwest. In deeper part below 110 meters, it tends to show higher value to the depth, and divided by complicated tectonic lines.

4) Metal factor

The low resistivity and high chargeability zone extracted in the area below 110 meters level show the maximum value around the survey lines g(No.7), h(No.10), i(No.13), j(No.16), and k(No.16), trending its structure northeast to southwest.

The highest metal factor 1,222 is around seen around the survey line k, points No.15 and 16. The low resistivity and high charge rate zone is corresponded with a part of the northeast to southwest trending ground magnetic anomaly zone.

Figure II-2-1-78 shows the ground magnetic and IP anomaly zone as a summary of the IP survey.

The known existing ore deposits around the survey districts are accompanied with pyrrhotite, chalcopyrite, pyrite, and arsenopyrite, therefore both factors of the high magnetism, and low resistivity - high chargeability should be considered for the mineral prospecting. The potential area for such ores in the survey districts is the area around the survey lines g(No.7), h(No.10), i(No.13), j(No.16), and k(No.16),

It is presumed that the IP anomaly zone is of a platy shape, and situated from the depth of 110 meters to the deeper, trending northeast to southwest, dipping nearly vertical.

The magnetic anomaly zone and IP anomaly zone appear concordantly each other in the survey district, accordingly it is difficult to think these anomaly as graphite cases. However, the possibility of graphite is not completely negative, judging from the geological environment. In case the area contains some graphite thin layers, similar IP anomaly as same the case of some ores would appear.

In any event, it is necessary to confirm the rocks in the IP anomaly zone by drilling.

[Dipole Spacing=100m Dipole-Dipole Electrode Configuration]

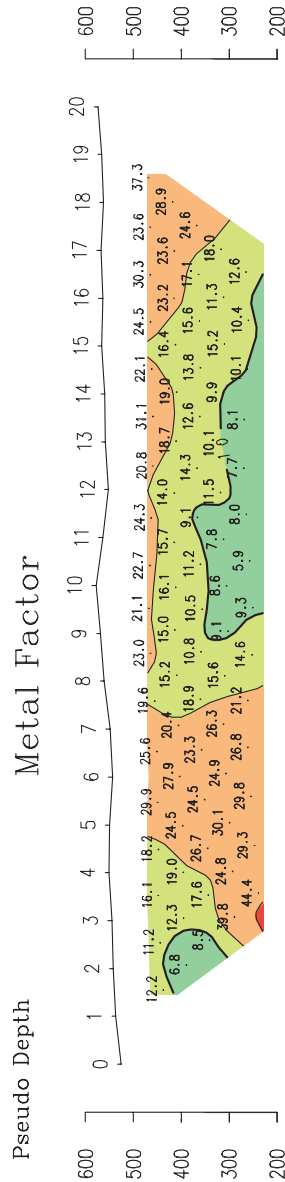
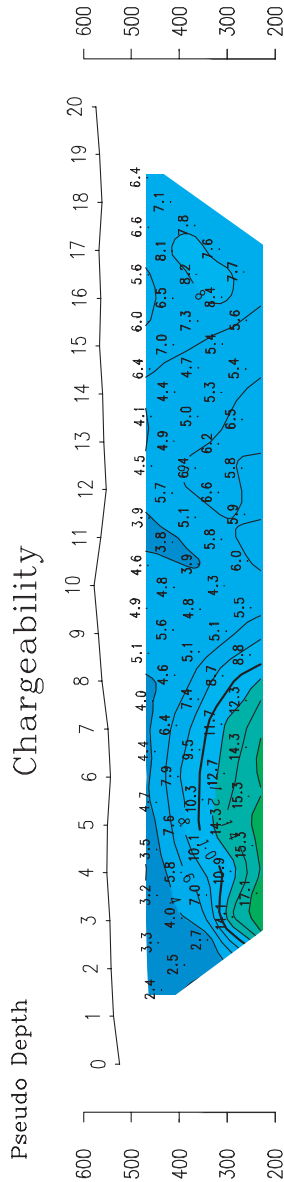
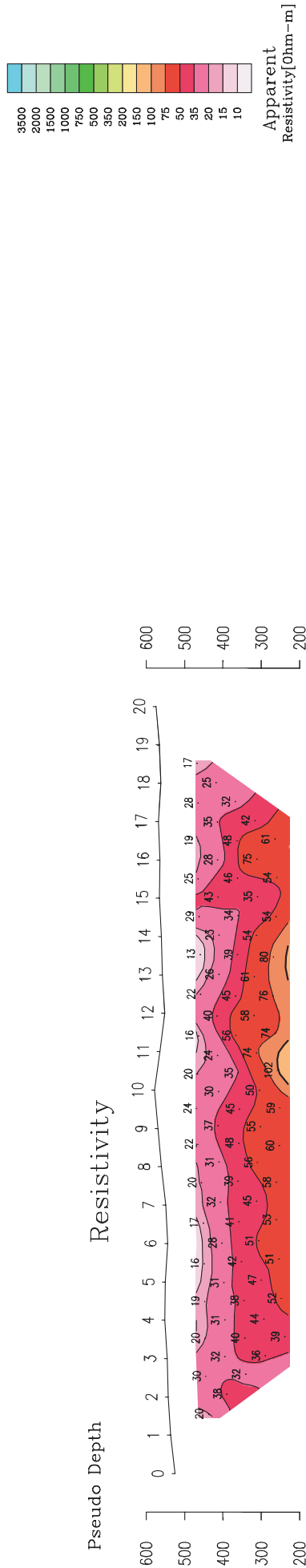


Fig.II-2-1-7 IP pseudo-sections at Azzouz area (a line)

[Dipole Spacing=100m Dipole-Dipole Electrode Configuration]

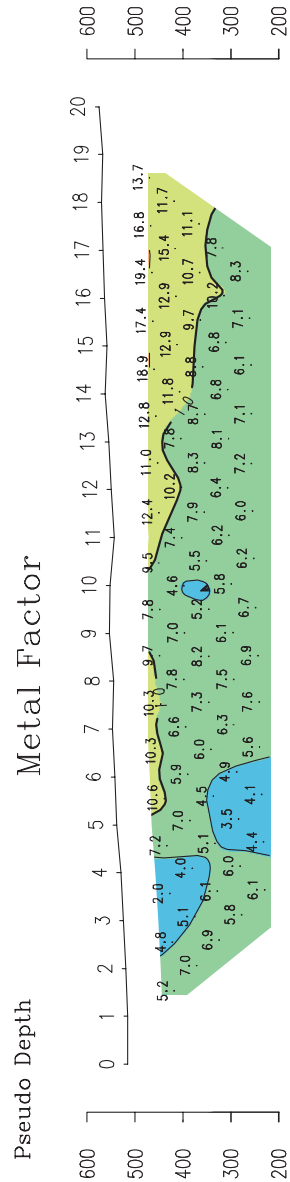
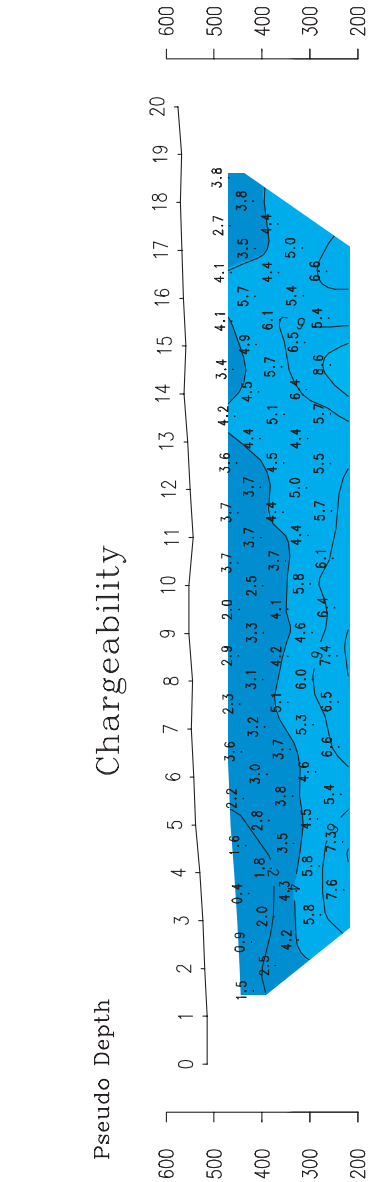
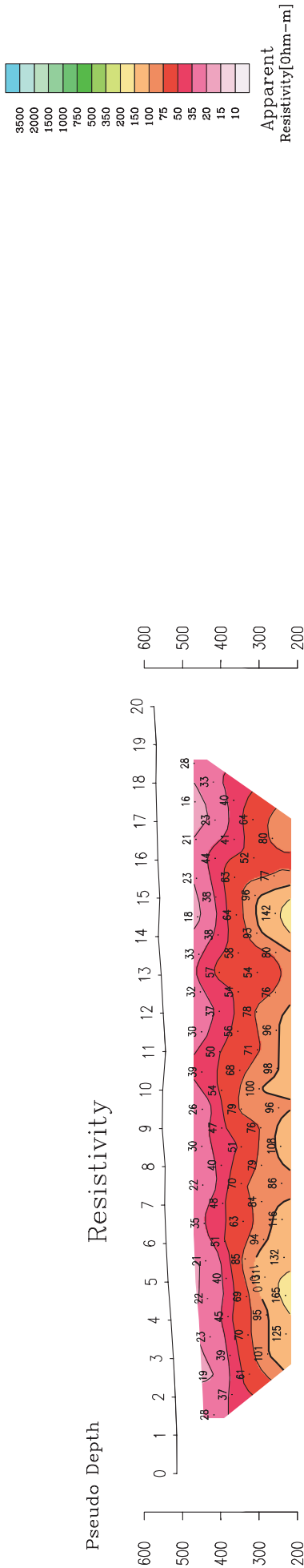


Fig-II-2-1-8 IP pseudo-sections at Azzouz area (b line)

[Dipole Spacing=100m Dipole-Dipole Electrode Configuration]

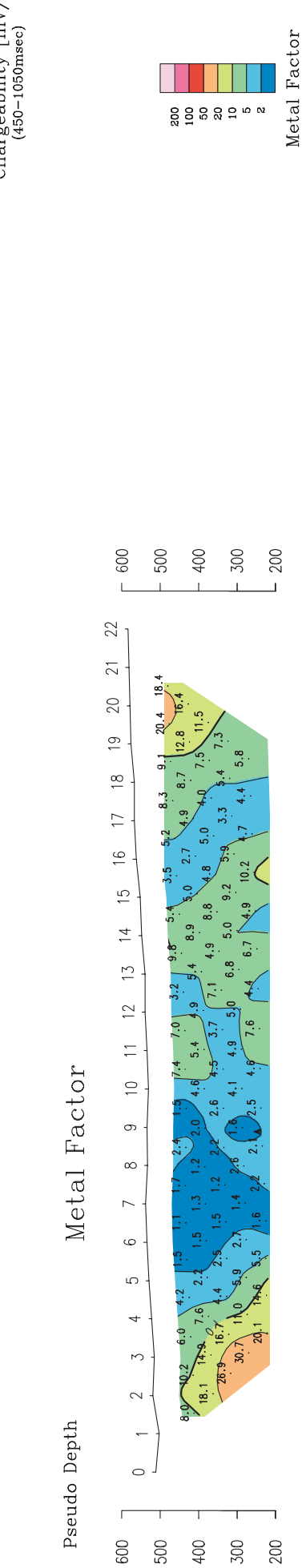
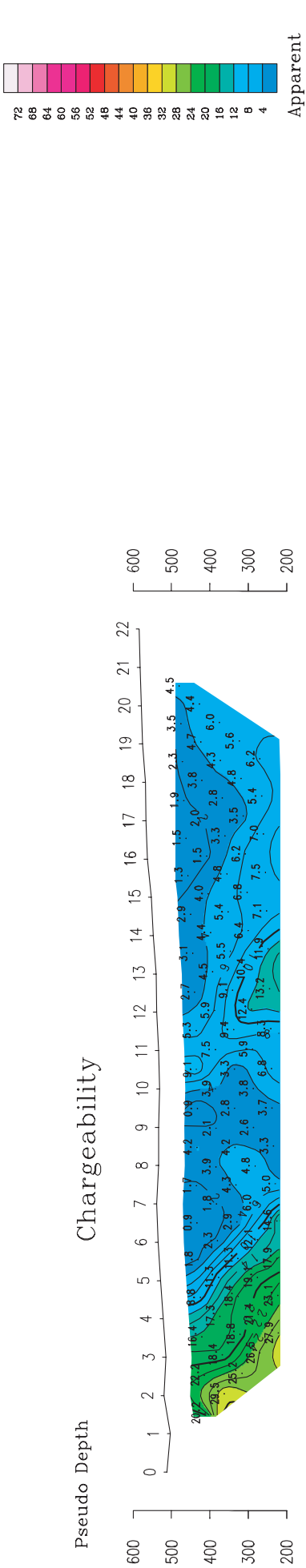
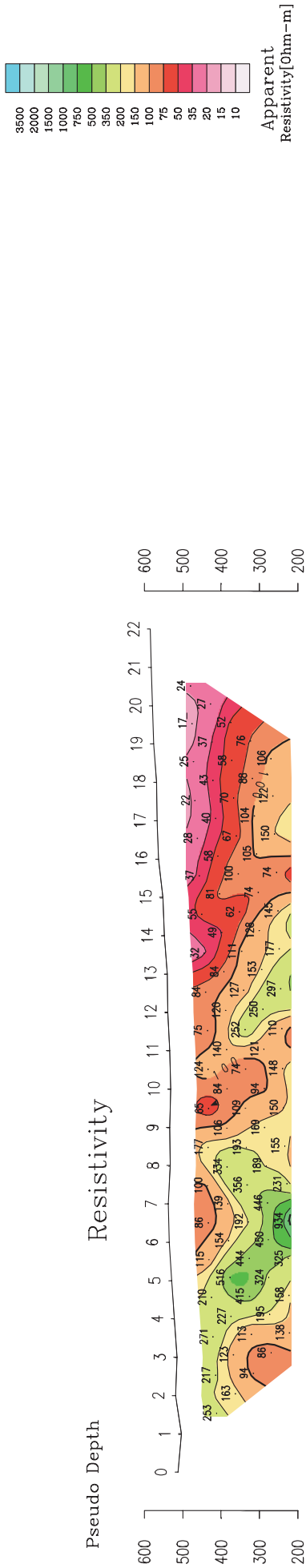


Fig.II-2-1-9 IP pseudo-sections at Azzouz area (c line)

[Dipole Spacing=100m Dipole-Dipole Electrode Configuration]

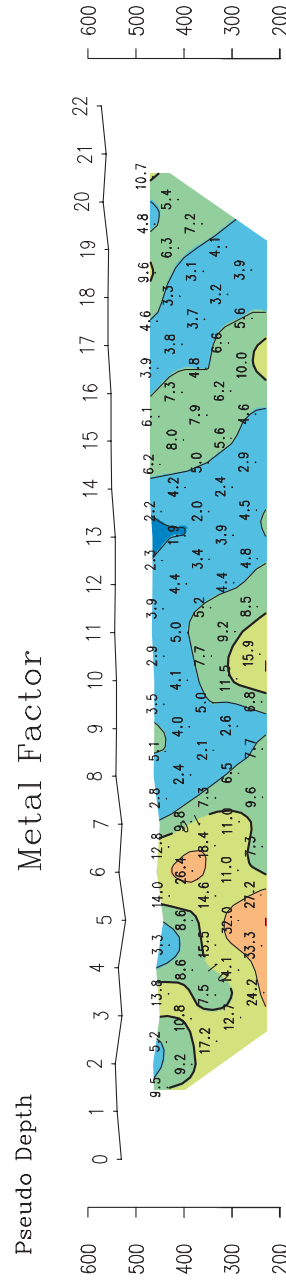
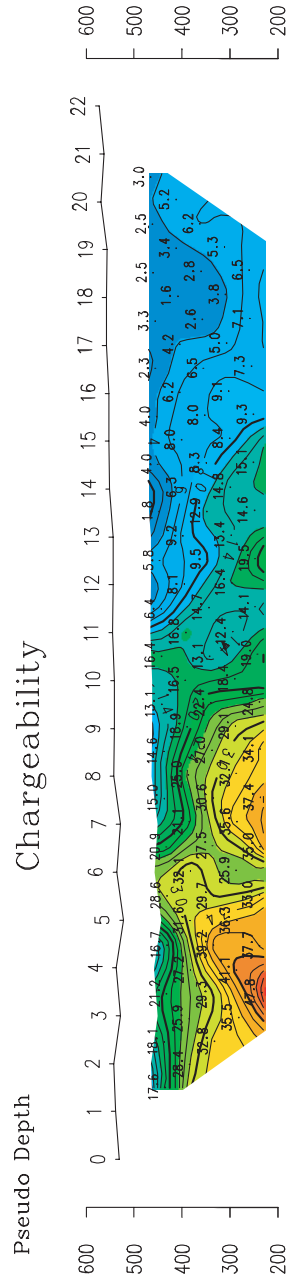
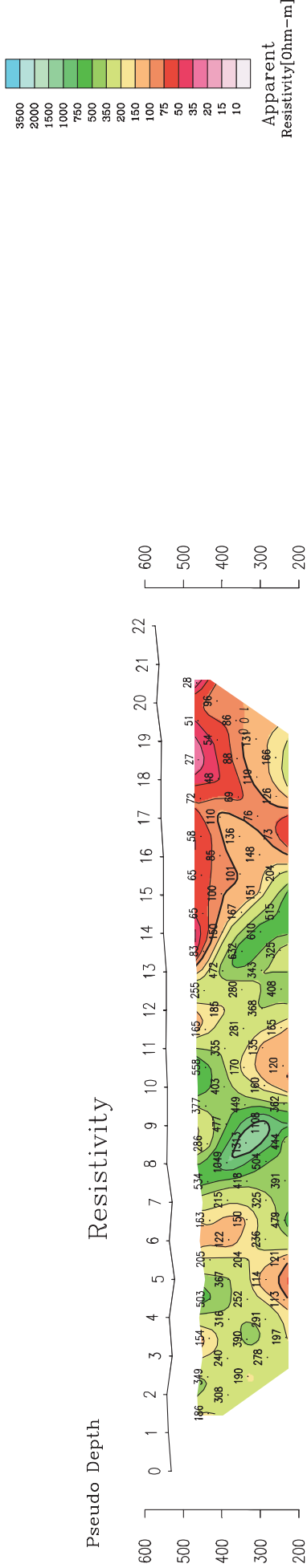


Fig.II-2-1-10 IP pseudo-sections at Azzouz area (d line)

[Dipole Spacing=100m Dipole-Dipole Electrode Configuration]

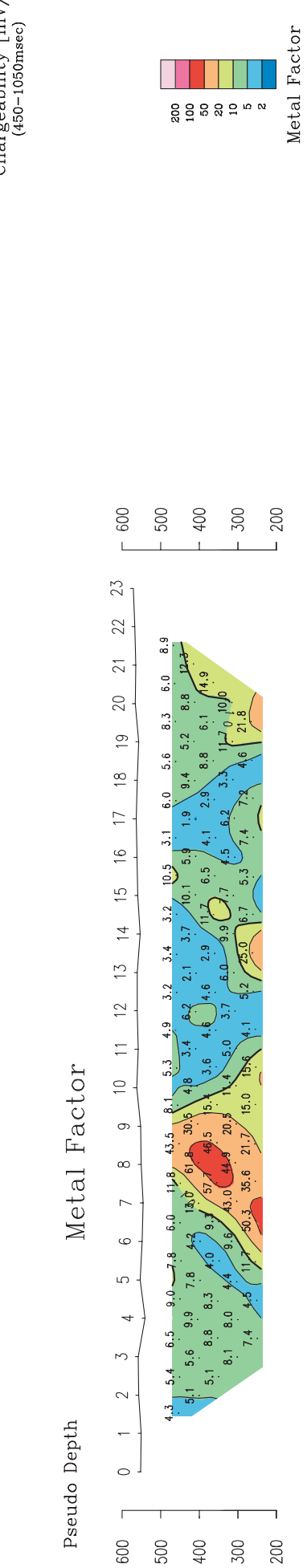
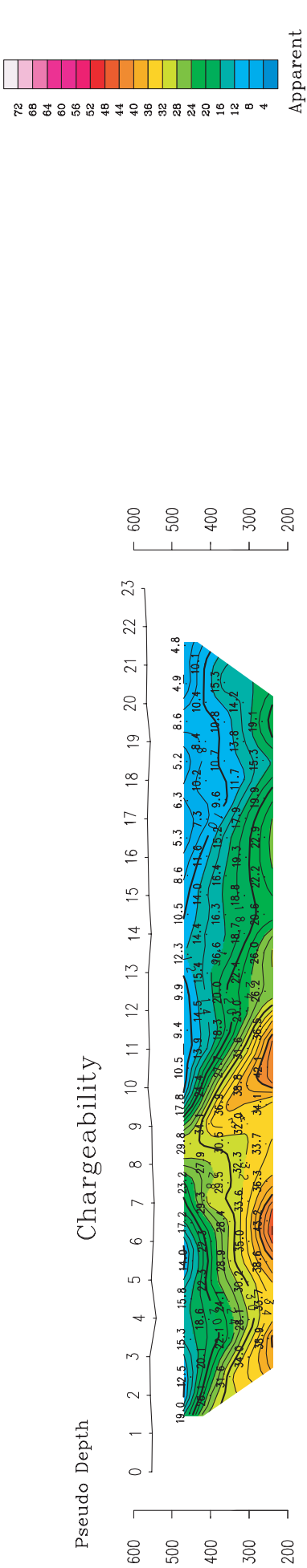
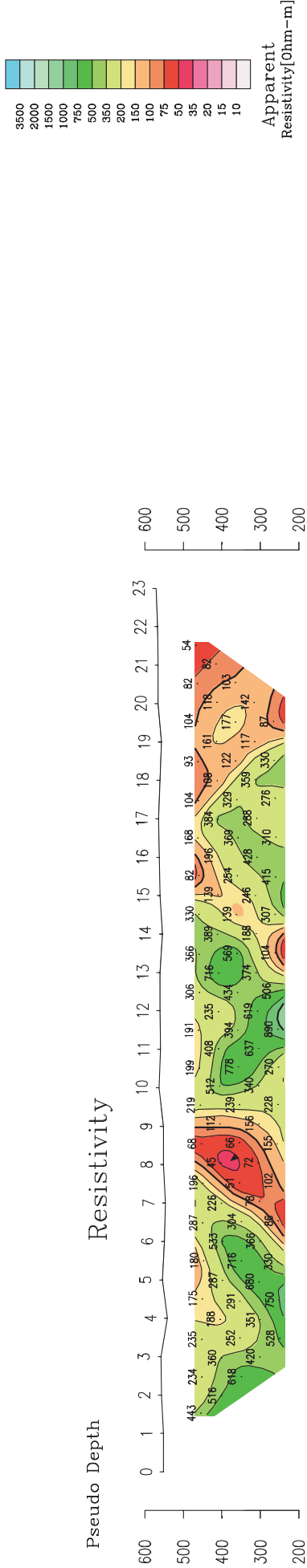


Fig.II-2-1-11 IP pseudo-sections at Azzouz area (e line)

[Dipole Spacing=100m Dipole-Dipole Electrode Configuration]

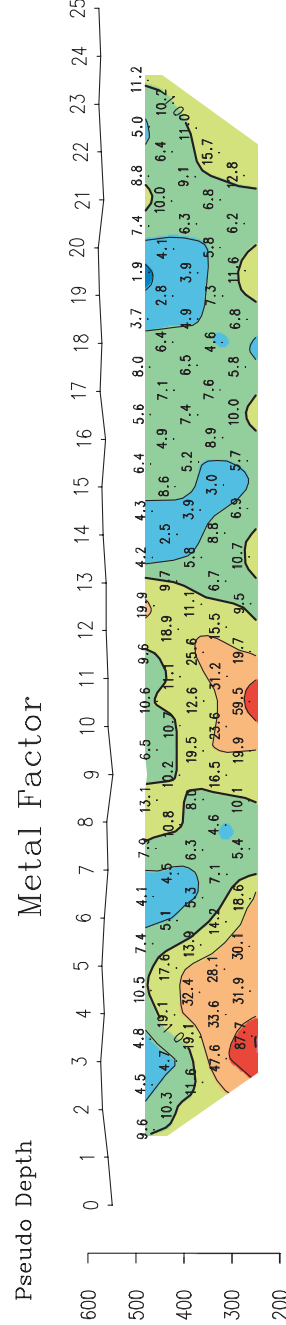
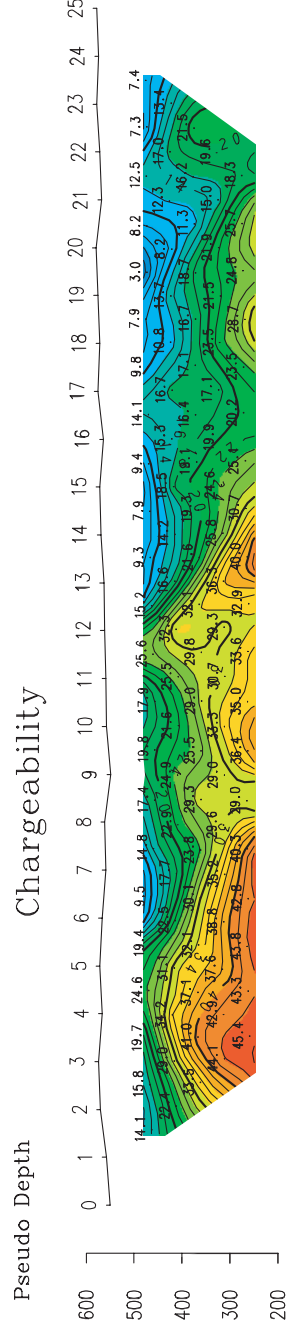
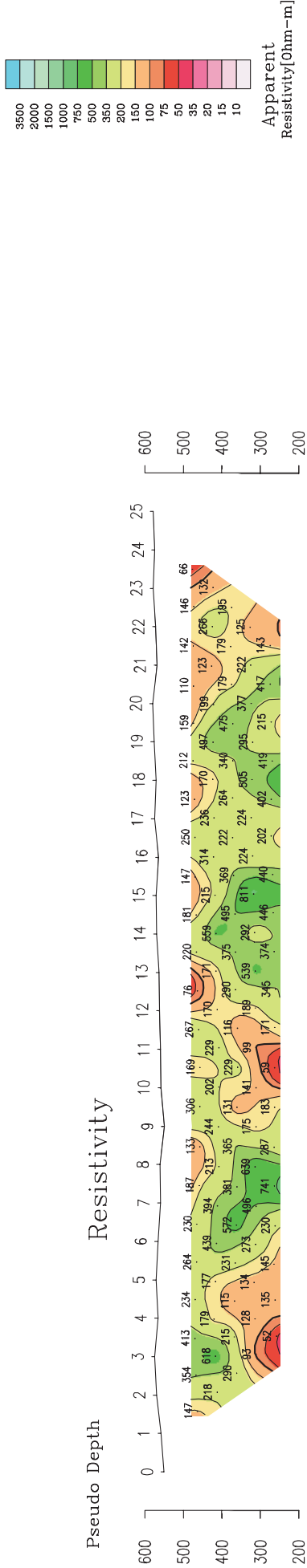


Fig.II-2-1-12 IP pseudo-sections at Azzouz area (f line)

[Dipole Spacing=100m Dipole-Dipole Electrode Configuration]

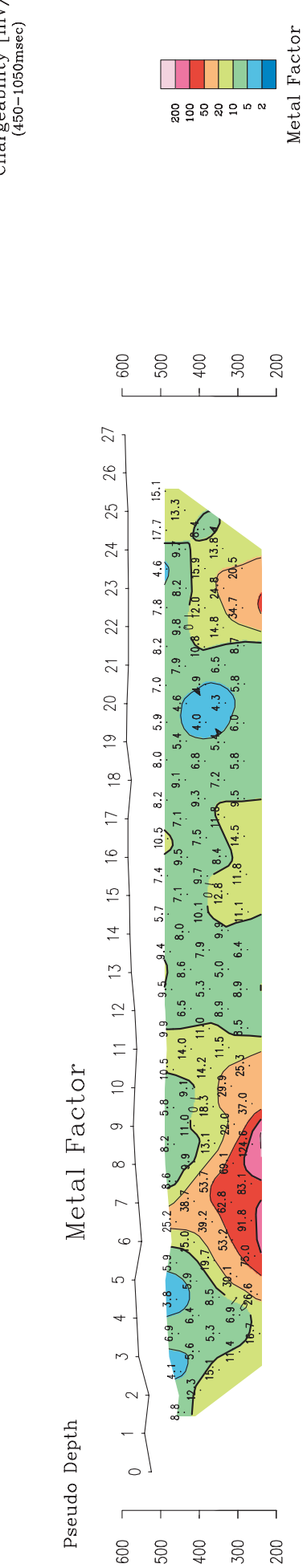
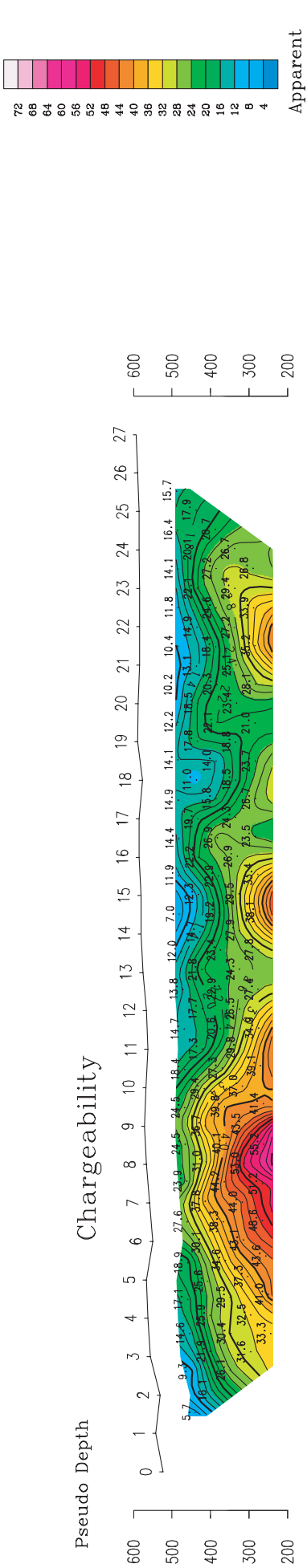
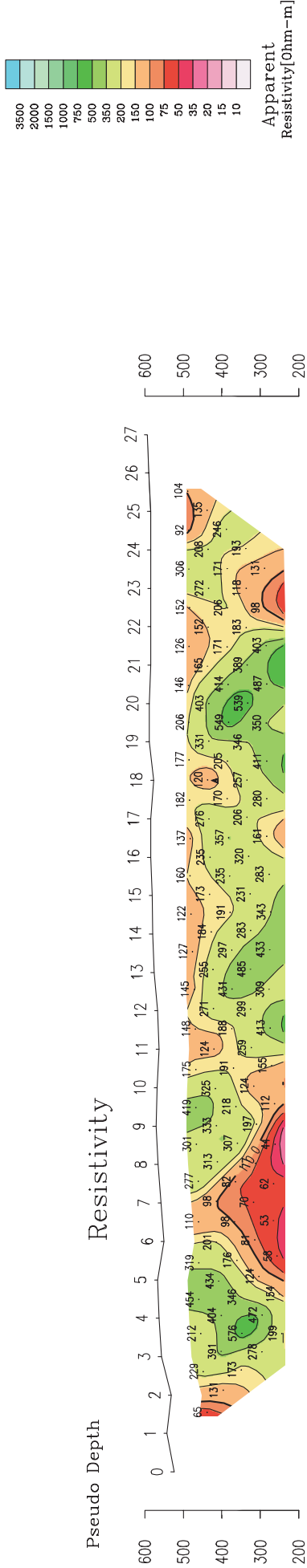


Fig.II-2-1-13 IP pseudo-sections at Azzouz area (g line)

[Dipole Spacing=100m Dipole-Dipole Electrode Configuration]

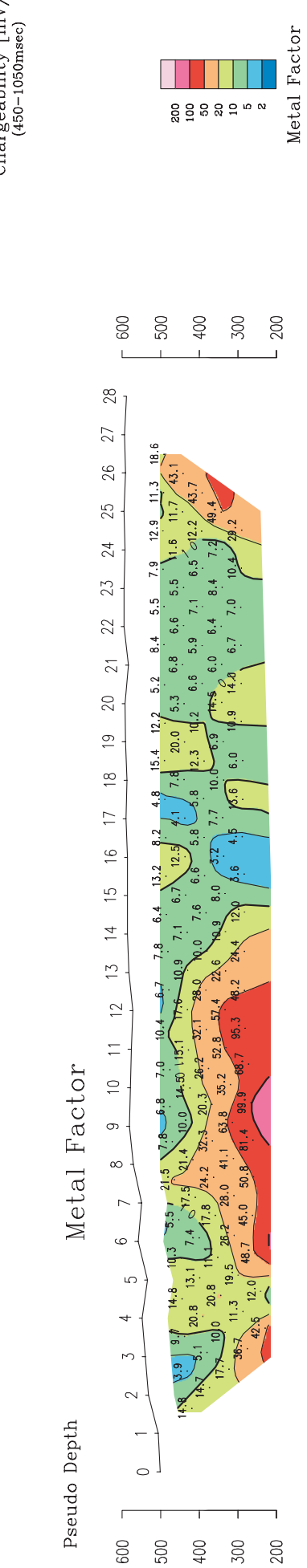
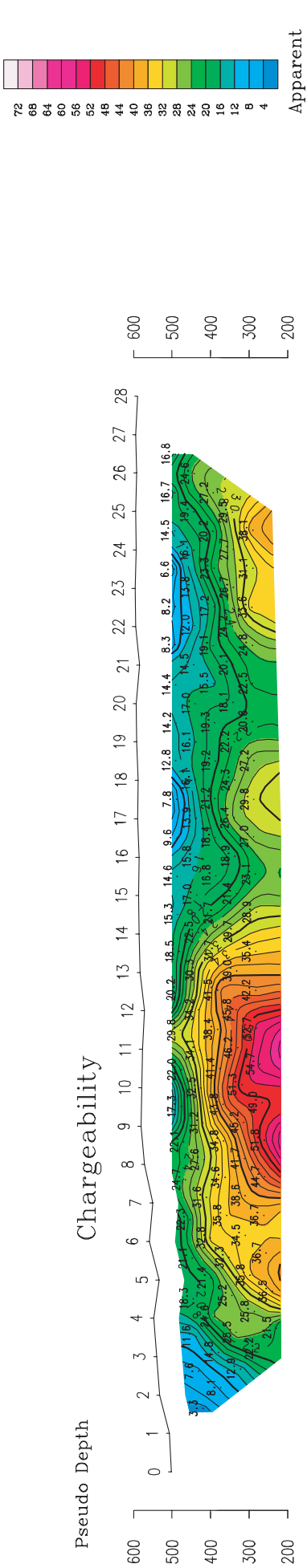
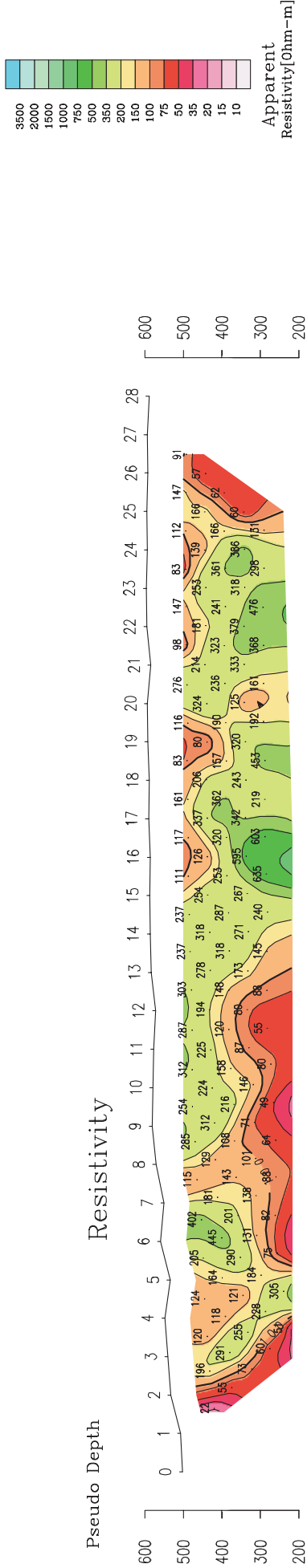


Fig.II-2-1-14 IP pseudo-sections at Azzouz area (h line)

[Dipole Spacing=100m Dipole-Dipole Electrode Configuration]

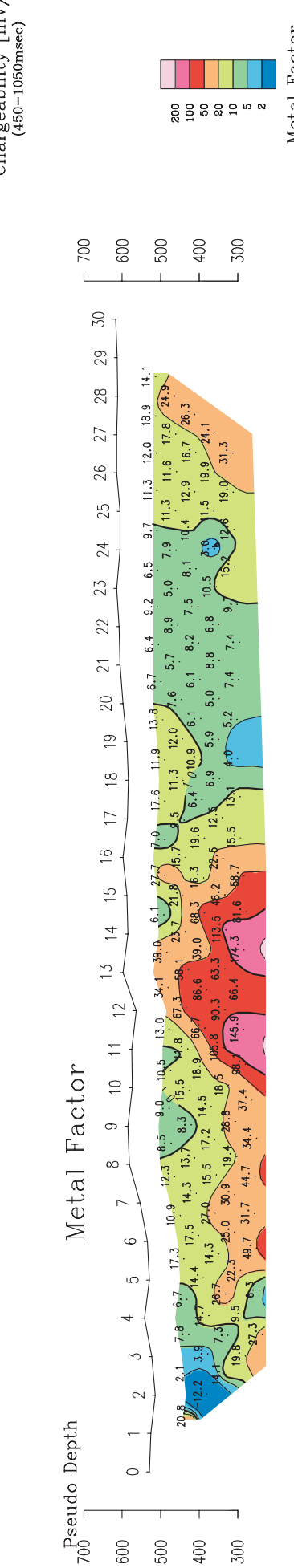
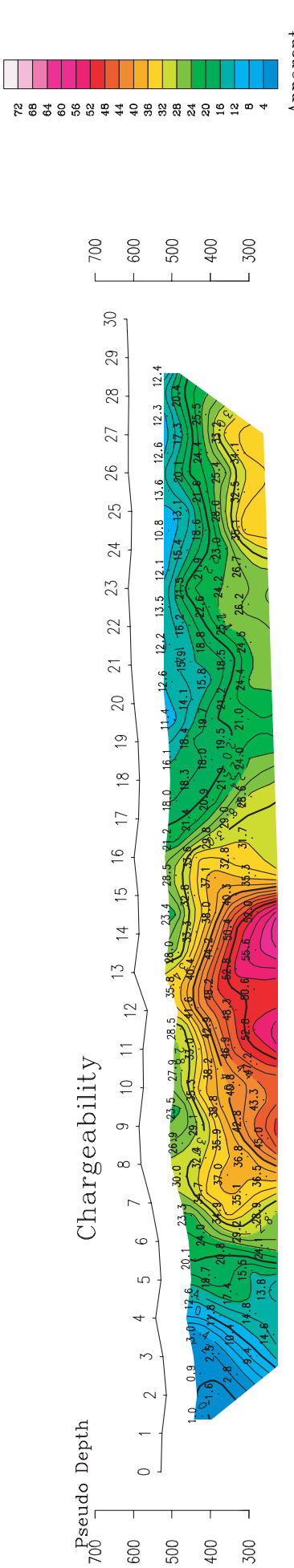
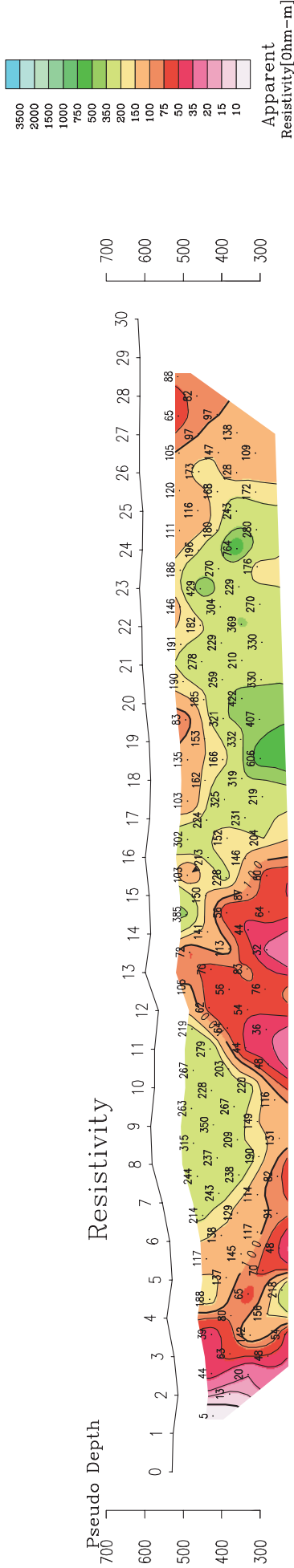
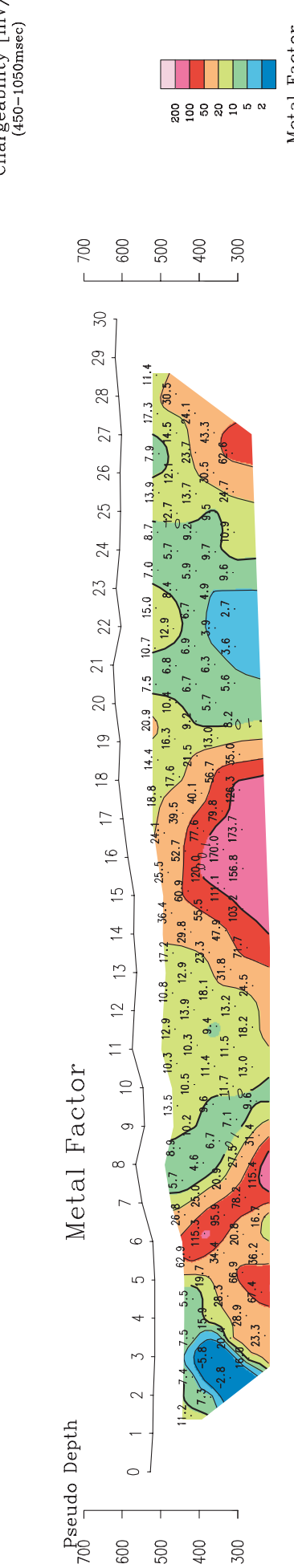
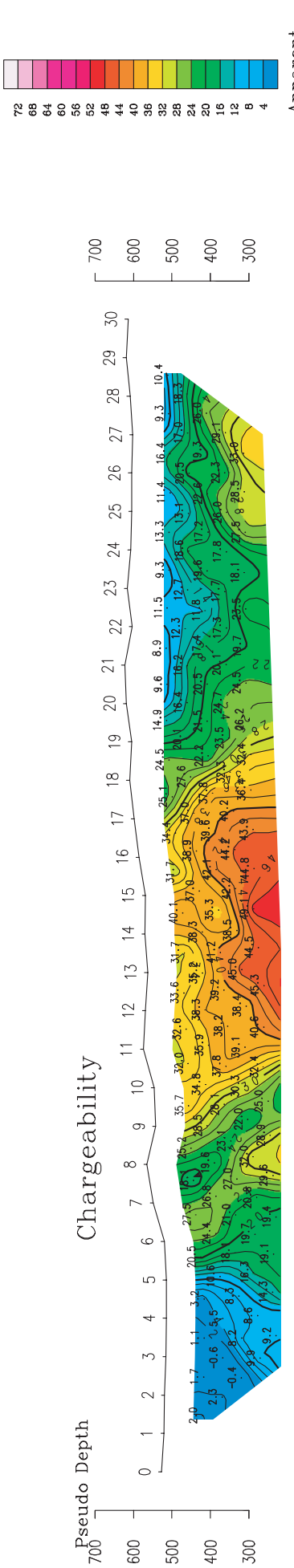
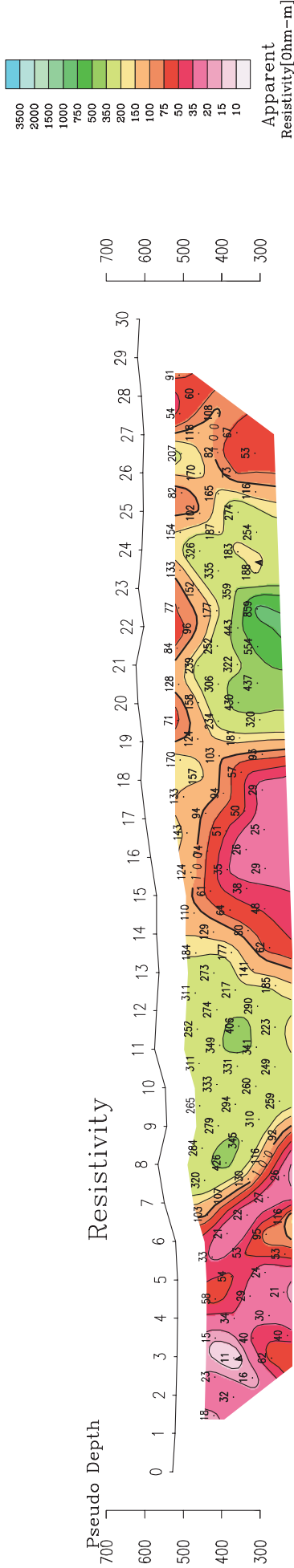


Fig.II-2-1-15 IP pseudo-sections at Azzouz area (i line)

[Dipole Spacing=100m Dipole-Dipole Electrode Configuration]



Metal Factor
250 0
(metres)

Fig.II-2-1-16 IP pseudo-sections at Azzouz area (j line)

[Dipole Spacing=100m Dipole-Dipole Electrode Configuration]

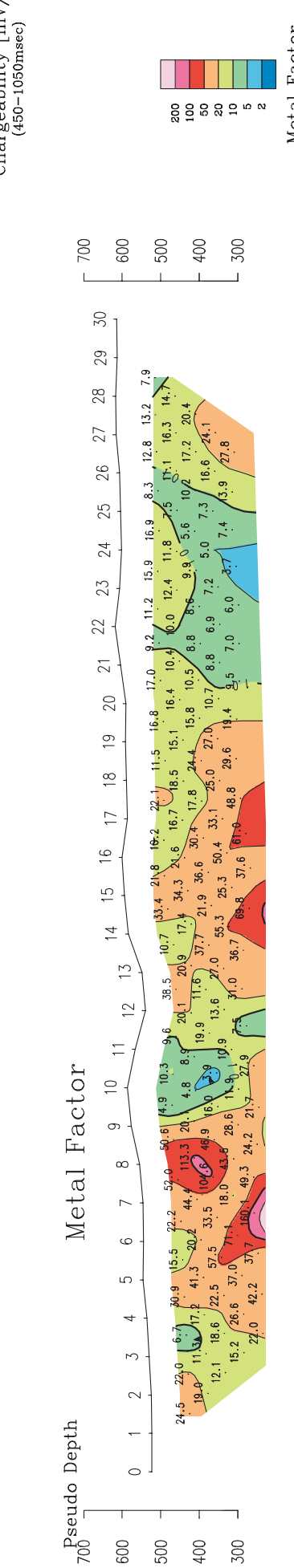
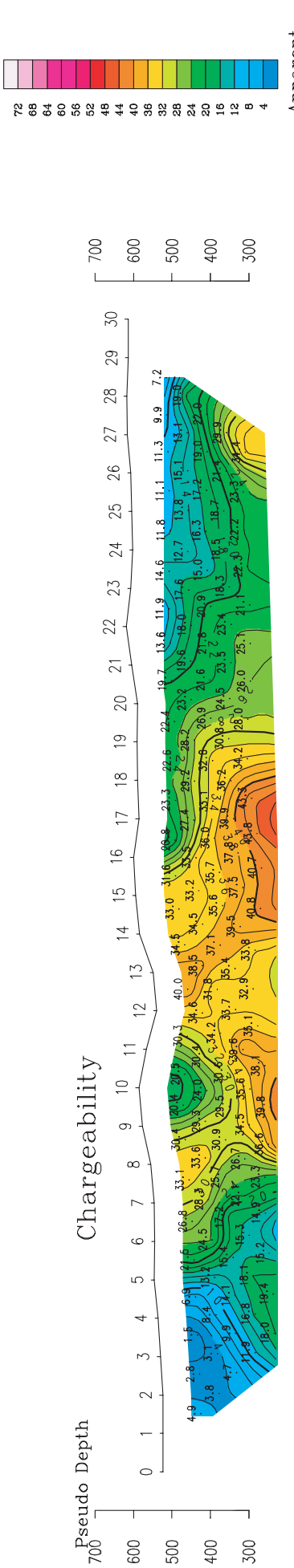
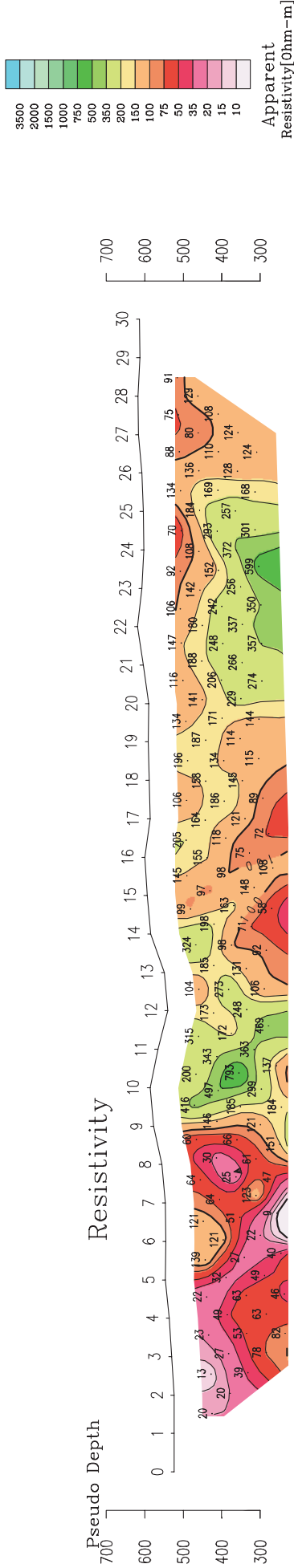


Fig.II-2-1-17 IP pseudo-sections at Azzouz area (k line)

[Dipole Spacing=100m Dipole-Dipole Electrode Configuration]

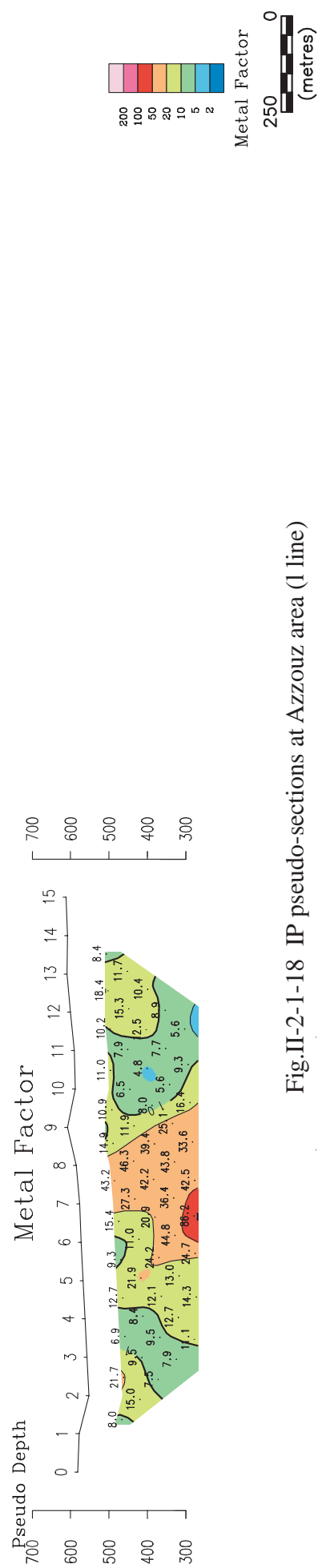
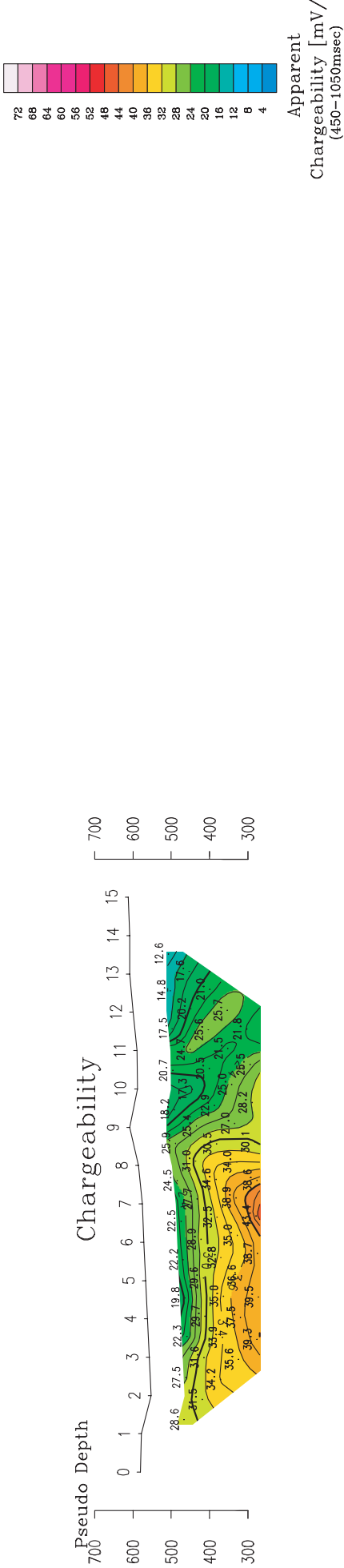
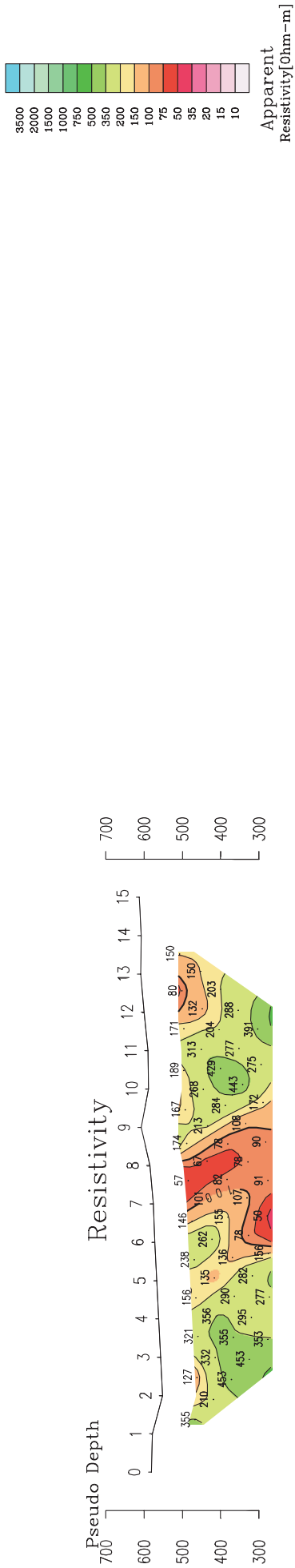


Fig.II-2-1-18 IP pseudo-sections at Azzouz area (1 line)

[Dipole Spacing=100m Dipole-Dipole Electrode Configuration]

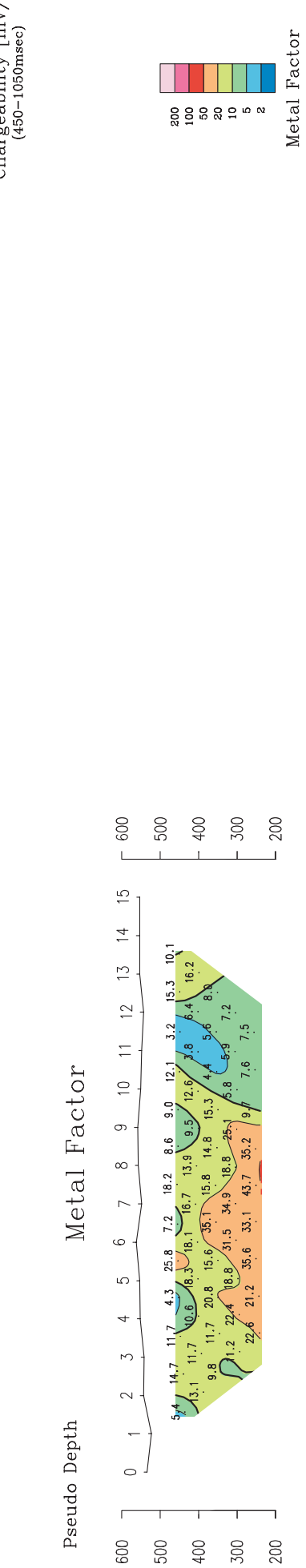
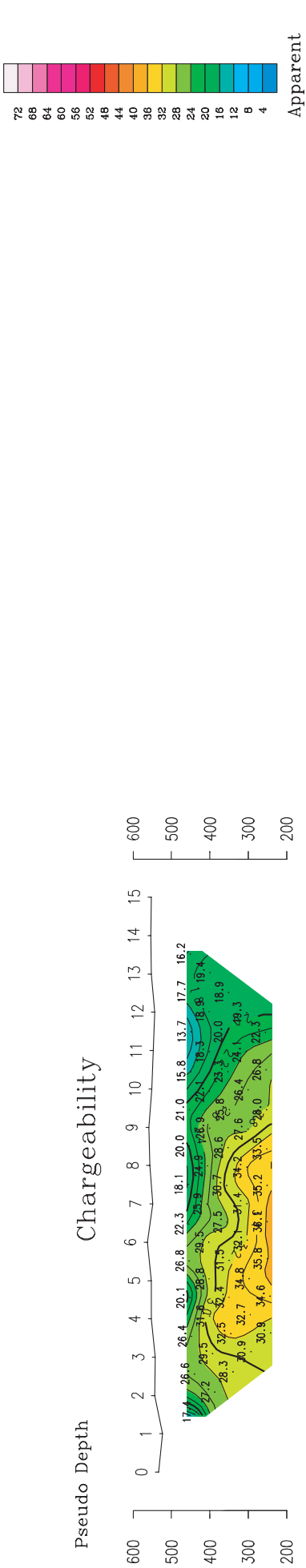
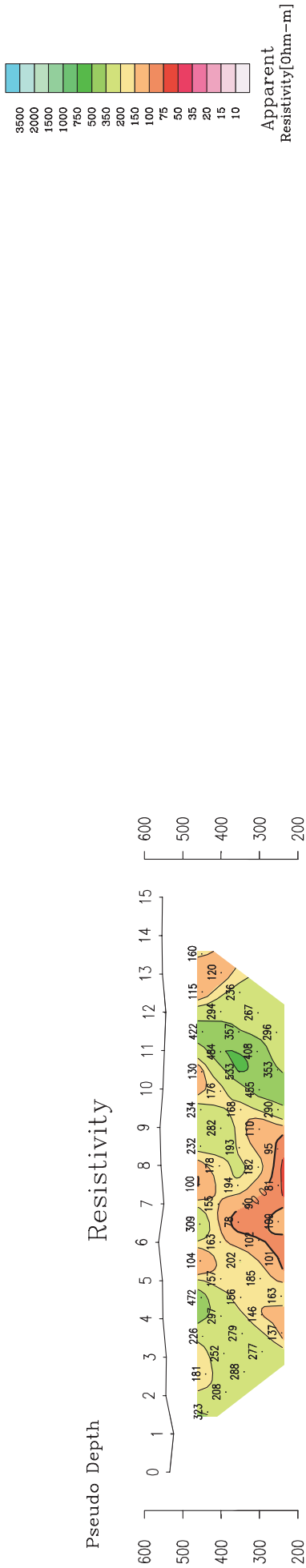


Fig.II-2-1-19 IP pseudo-sections at Azzouz area (m line)

[Dipole Spacing=100m Dipole--Dipole Electrode Configuration]

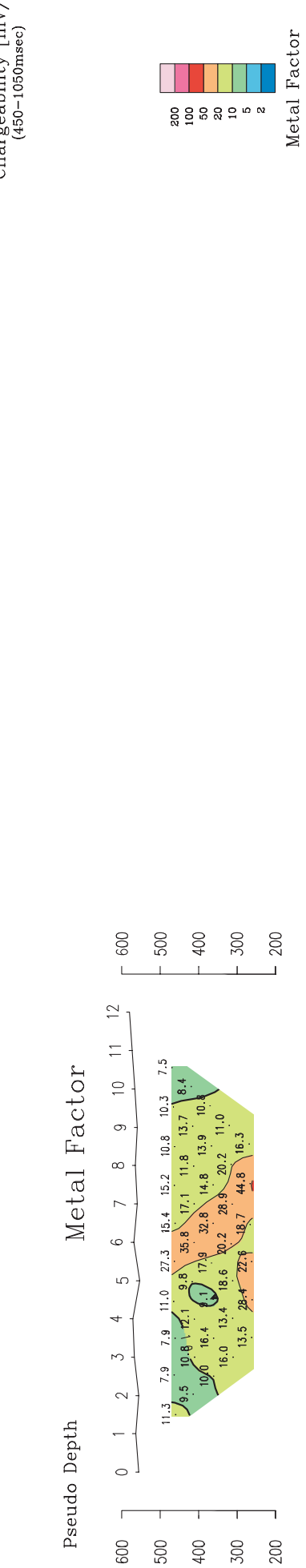
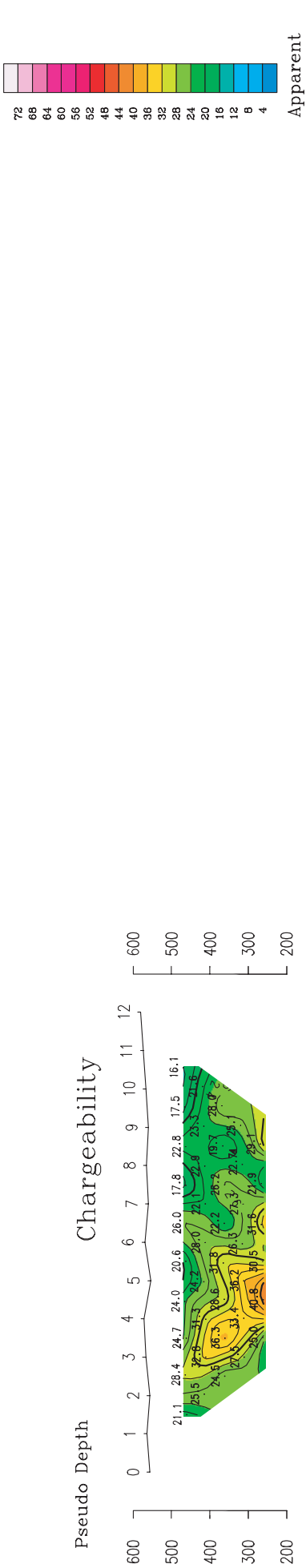


Fig.II-2-1-20 IP pseudo-sections at Azzouz area (n line)

[Dipole Spacing=100m Dipole-Dipole Electrode Configuration]

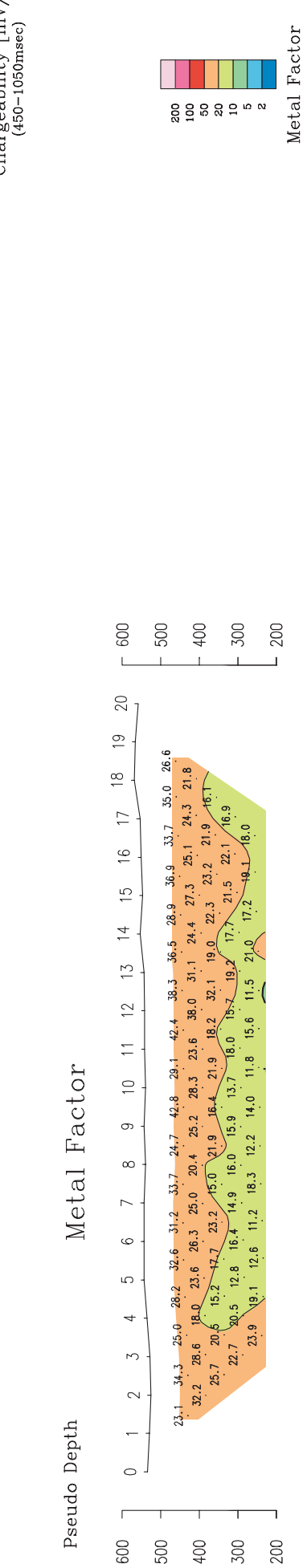
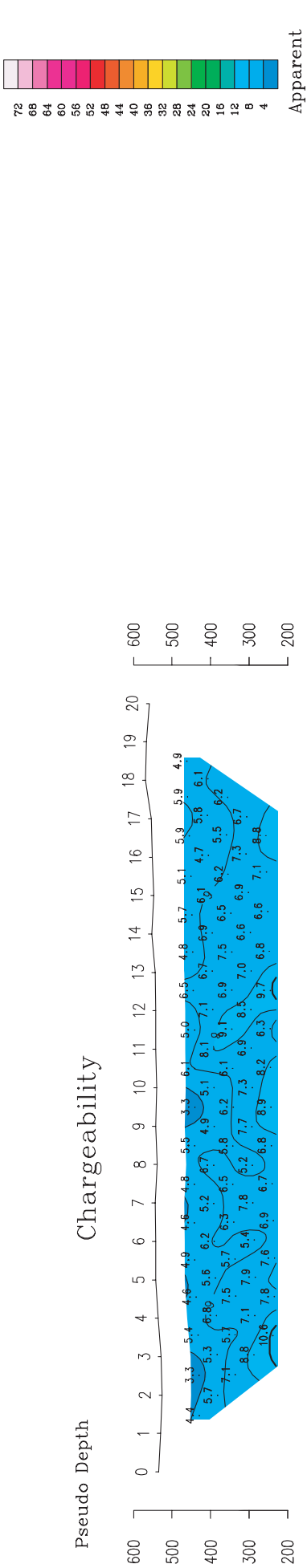
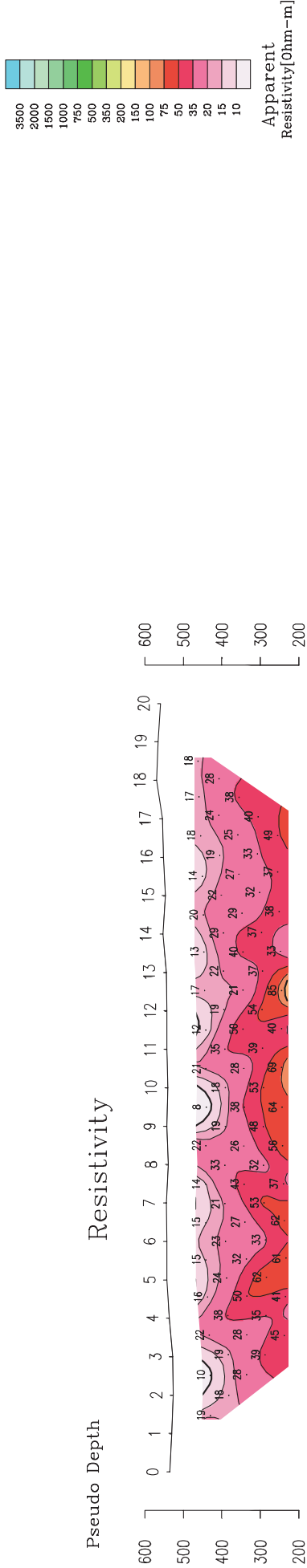


Fig.II-2-1-21 Ip pseudo-sections at azzouz area (o line)

[Dipole Spacing=100m Dipole-Dipole Electrode Configuration]

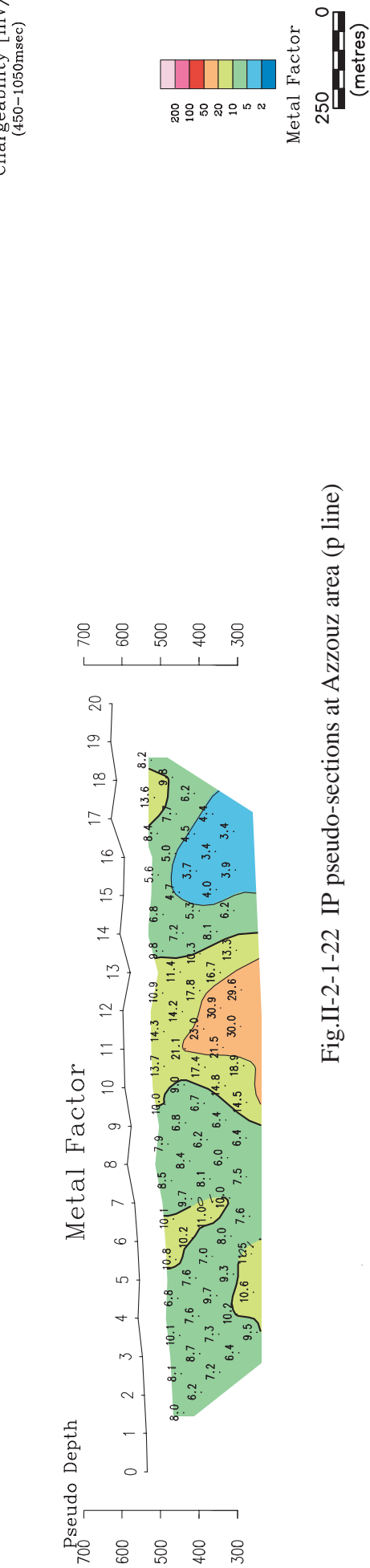
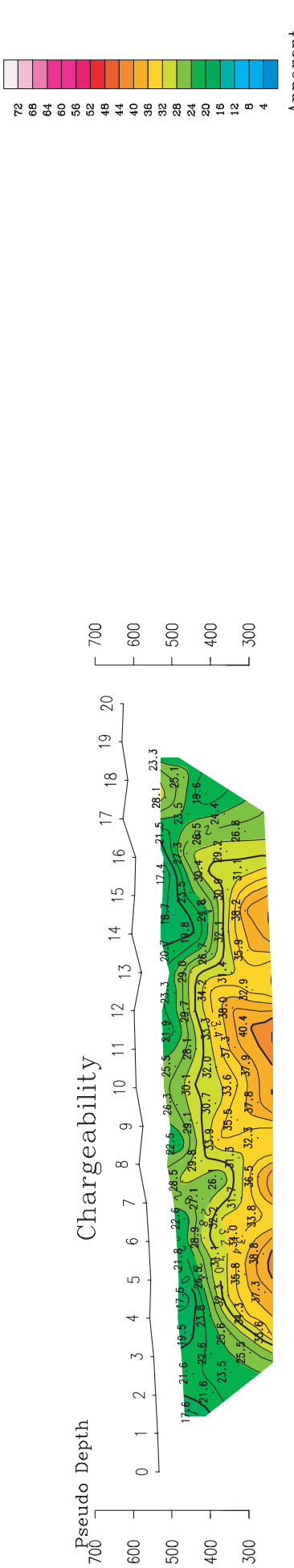
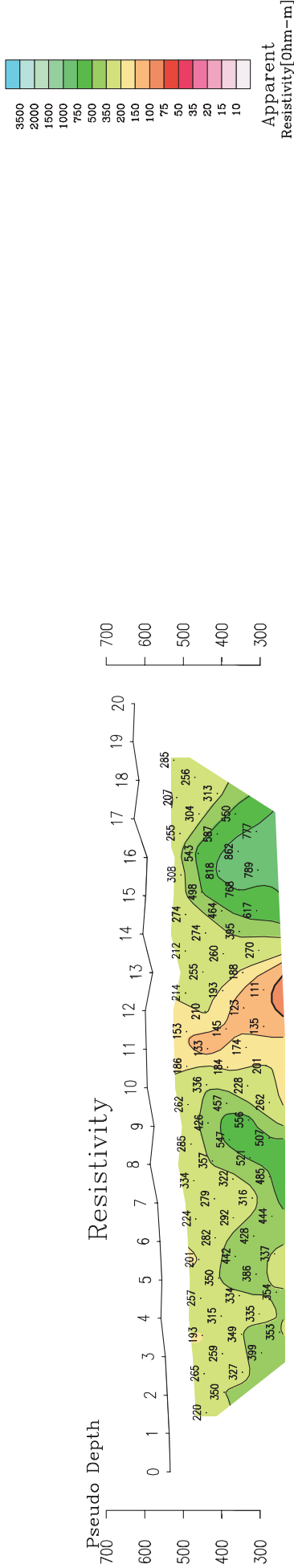


Fig.II-2-1-22 IP pseudo-sections at Azzouz area (p line)

[Dipole Spacing=100m Dipole-Dipole Electrode Configuration]

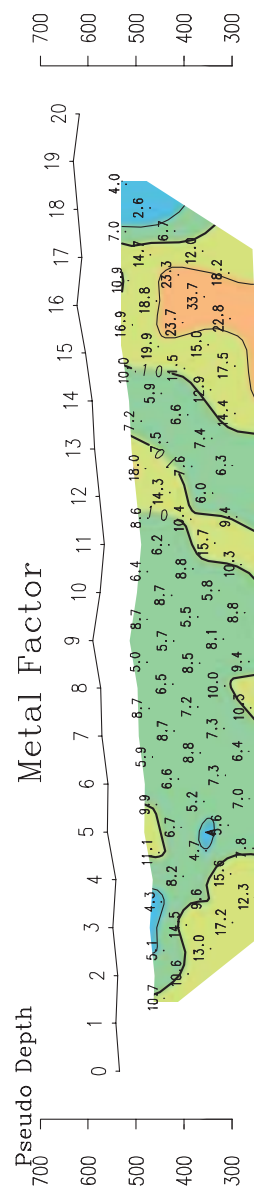
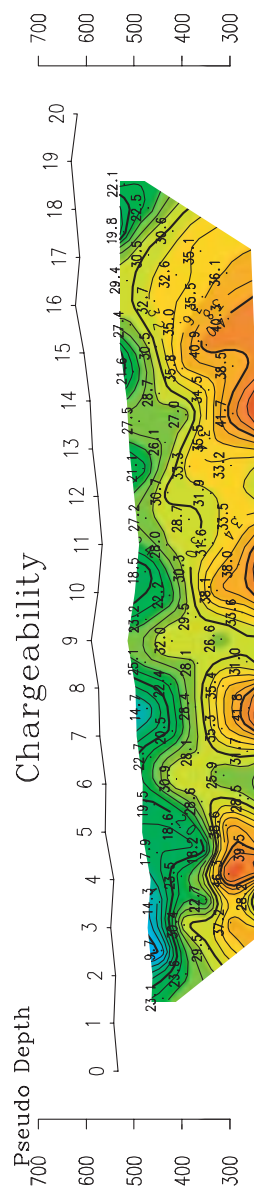
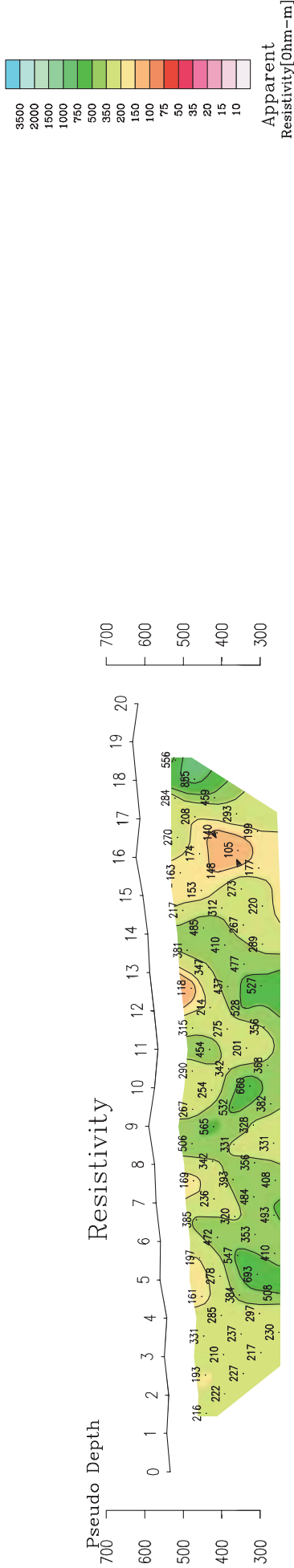


Fig.II-2-1-23 IP pseudo-sections at Azzouz area (q line)

[Dipole Spacing=100m Dipole-Dipole Electrode Configuration]

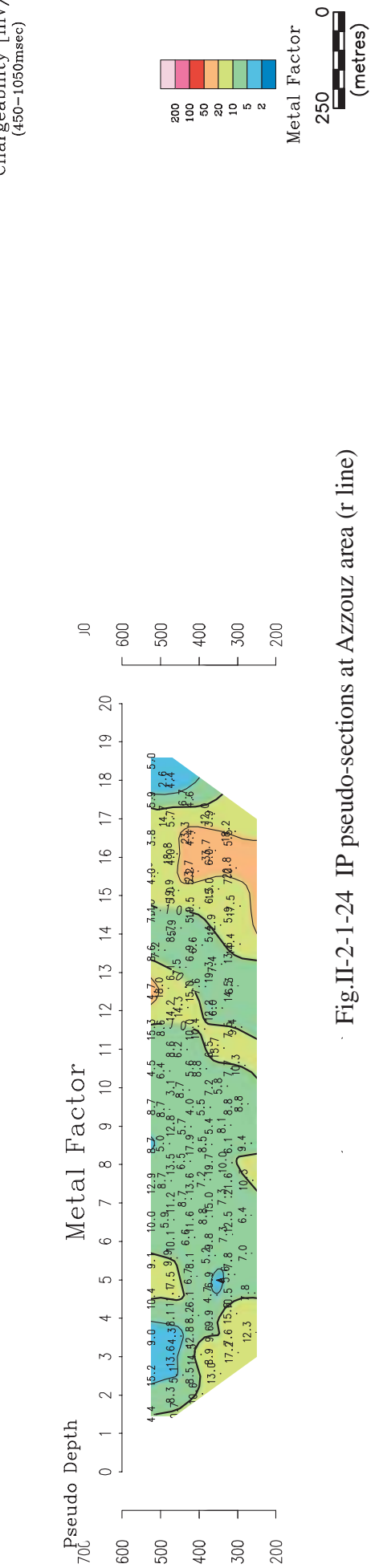
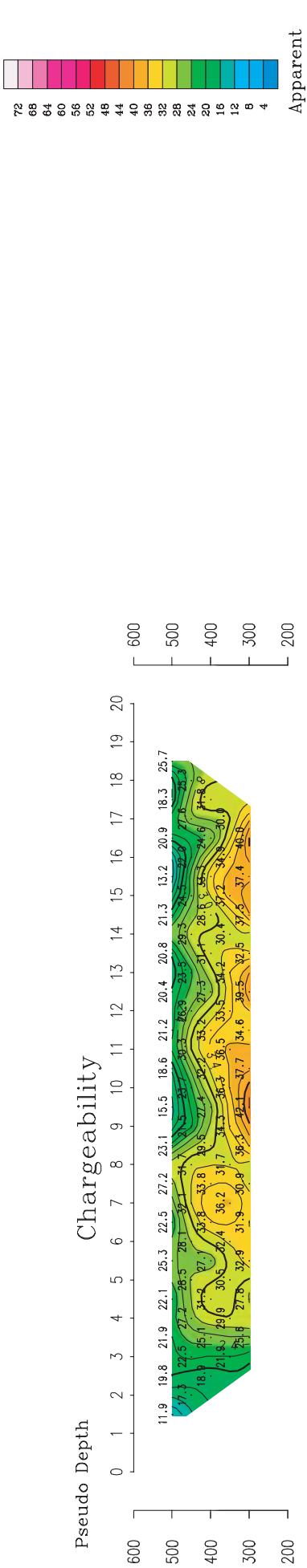
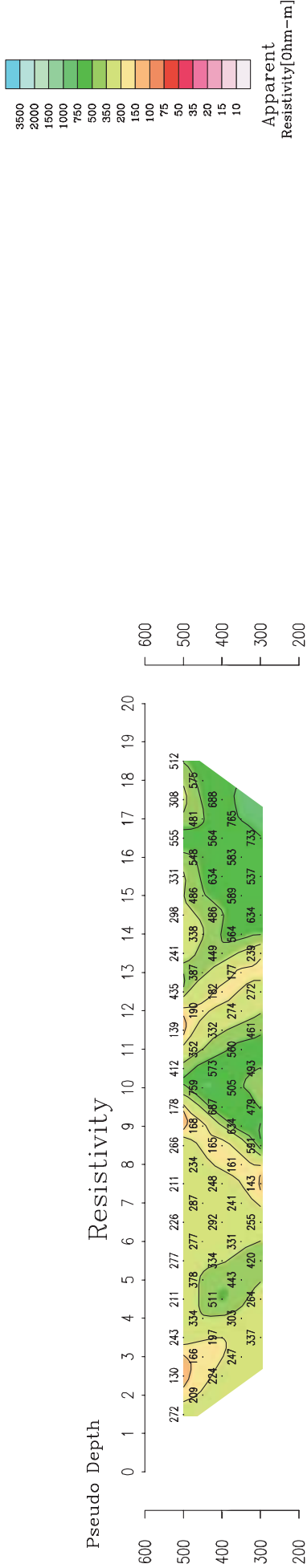


Fig.II-2-1-24 IP pseudo-sections at Azzouz area (r line)

[Dipole Spacing=100m Dipole-Dipole Electrode Configuration]

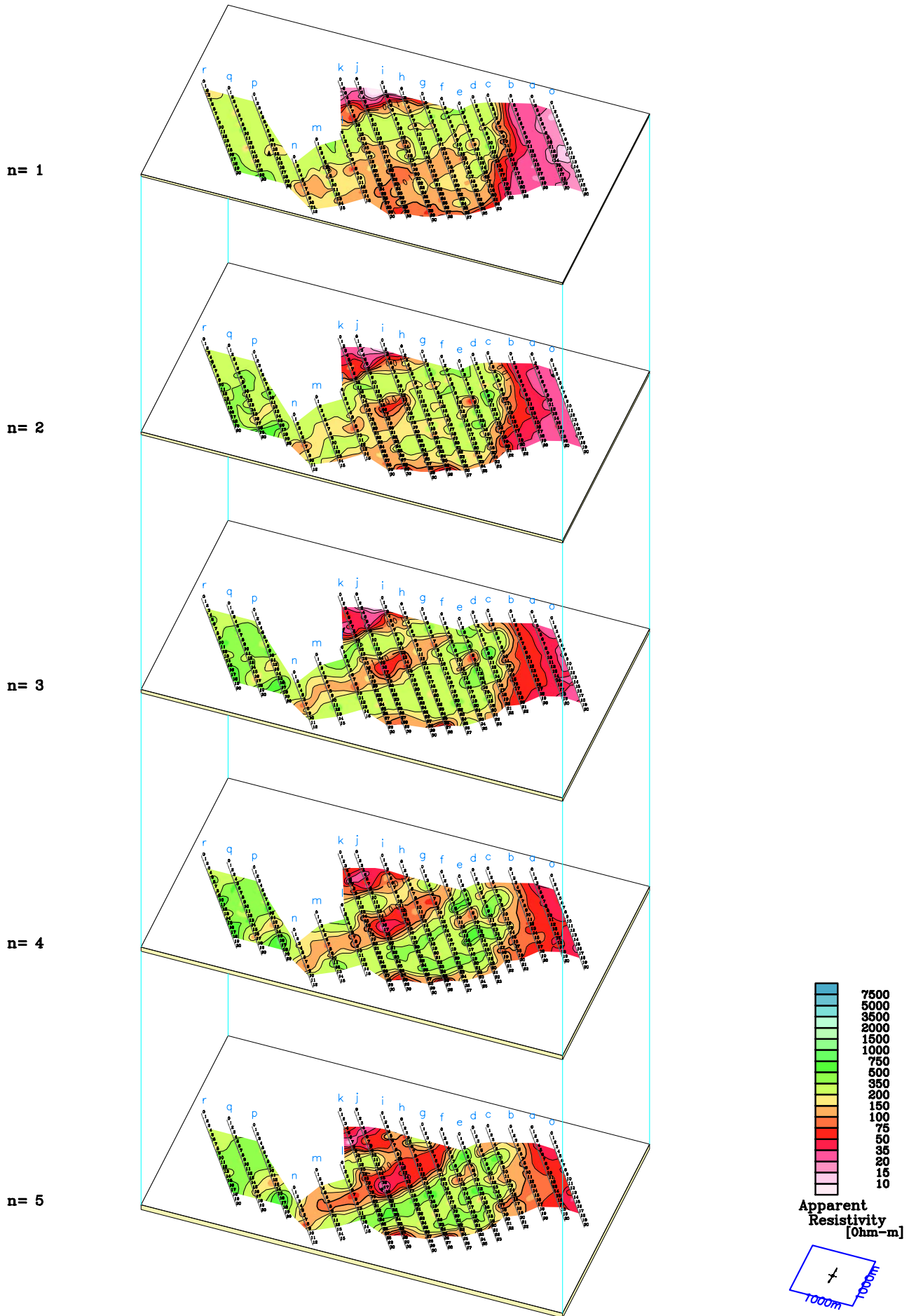


Fig.II-2-1-25 Plane map of apparent resistivity at Azzouz area

[Dipole Spacing=100m Dipole-Dipole Electrode Configuration]

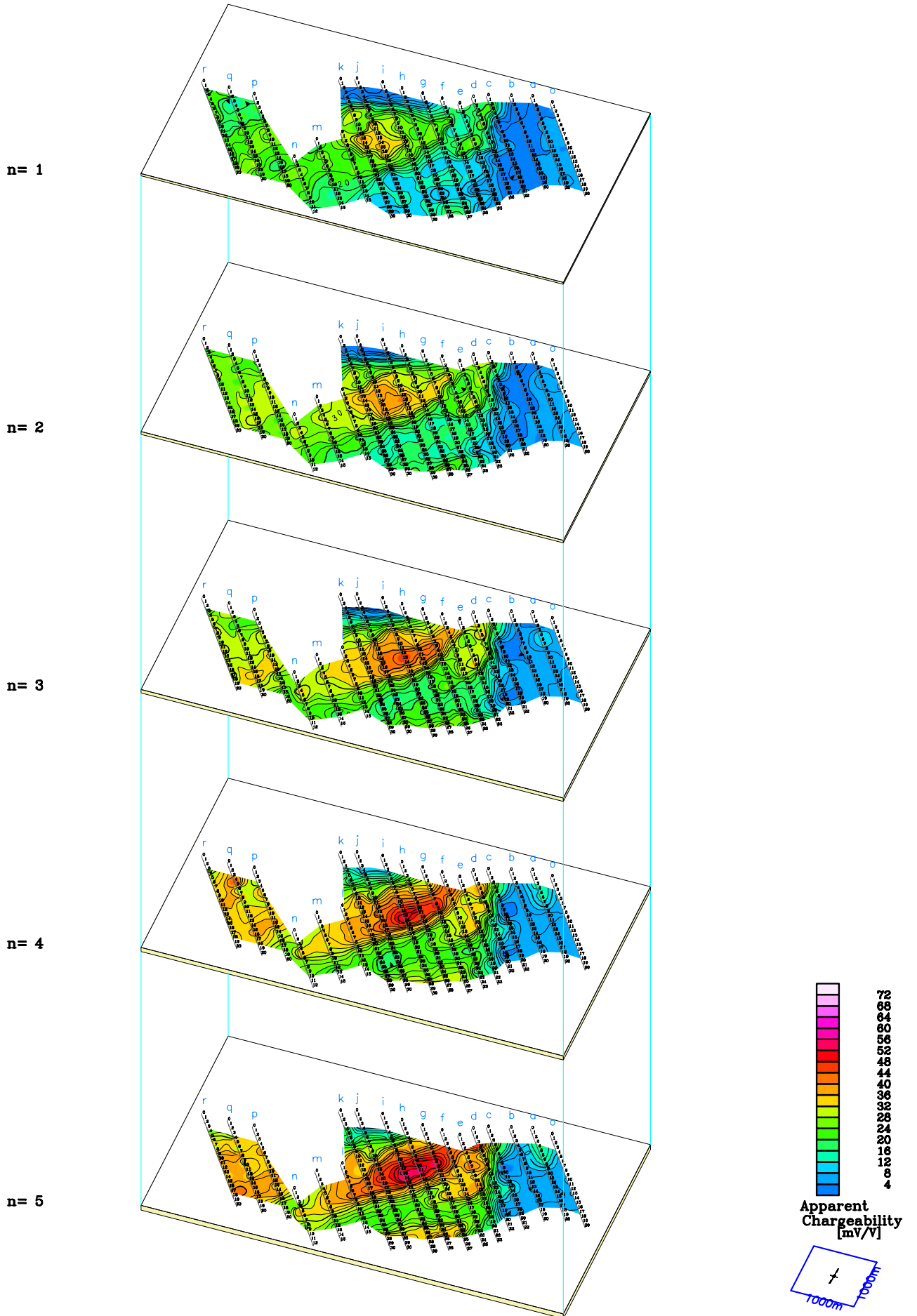


Fig.II-2-1-26 Plane map of apparent chargeability at Azzouz area

[Dipole Spacing=100m Dipole-Dipole Electrode Configuration]

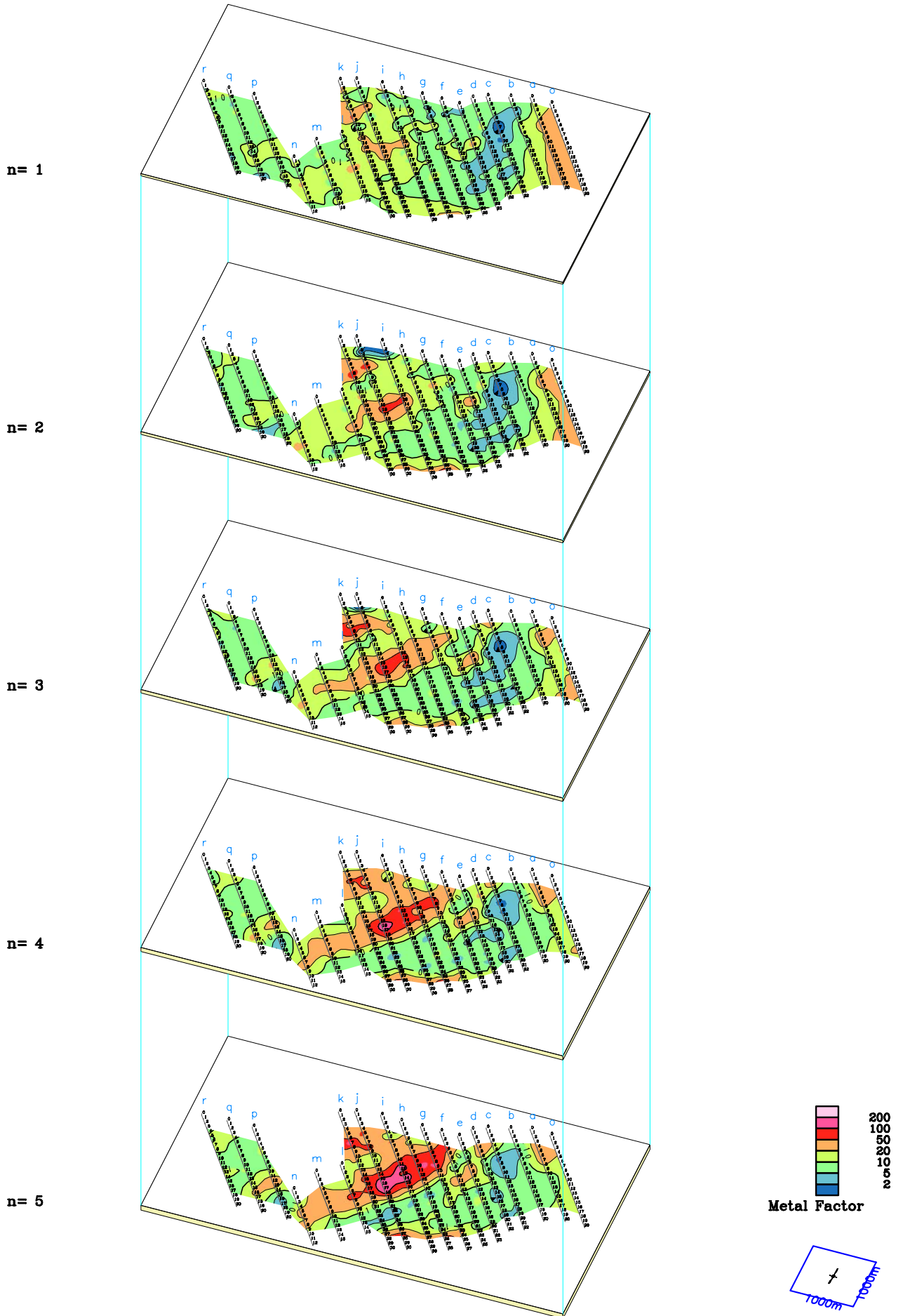


Fig.II-2-1-27 Plane map of metal factor at Azzouz area